ELSEVIER

Coordination Chemistry Reviews
147 (1996) 41–86

COORDINATION CHEMISTRY REVIEWS

Azaporphyrins: structure of the reaction centre and reactions of complex formation [1]

Pavel A. Stuzhin *, Ol'ga G. Khelevina

State Academy of Chemical Technology, RF-153460 Ivanovo, Russia

Received 21 March 1994; in revised form 10 August 1994

Contents

* Corresponding author.

[1] Dedicated to the 65th birthday of Professor Boris Dmitrievitch Berezin.

SSDI 0010-8545(94)01126-5

Abstract

X-ray, spectral (UV–visible, nuclear magnetic resonance and photoelectron spectroscopy) data and quantum-chemical calculation results for porphyrins, phthalocyanines and azaporphyrins are compared and conclusions about the influence of aza substitution on the geometry of CN skeleton and on the state of N—H bonds in porphyrin-type ligands are made. The studies of kinetics of metal ion incorporation in azaporphyrins are reviewed and the effect of the ligand structure, nature of metal salt and solvent on the complex formation reaction is discussed.

Keywords: Porphyrins; Phthalocyanines; Azaporphyrins; Complex formation

List of abbreviations

Macrocyclic ligands and their complexes

H_2AP	azaporphyrins
H_2Chl	chlorophyllic acid a
H_2DAP	*trans*-diazaporphine[1]
H_2MAP	monoazaporphine[1]
H_2MATBP	monoazatetrabenzoporphine
H_2NTBP	tribenzo(1-phenyl-2,3-naphthalo)porphine
H_2OEP	octaethylporphine
H_2P	porphine[1]
H_2TAP	tetraazaporphine[1]
H_2Pc	phthalocyanine[1]
H_2TATBP	triazatetrabenzoporphine[1]
H_2TBP	tetrabenzoporphine[1]
H_2TPP	*meso*-tetraphenylporphine
H_2TPrP	*meso*-tetra(*n*-propyl)porphine
MAP	metalloazaporphyrin
MP	metalloporphyrin
MTAP	metallotetraazaporphyrin[1]

[1] In the derivatives substituted in β positions of pyrrole rings or in annelated benzene rings the common depiction of the substituents and their number follow the abbreviations H_2TAPPh_8 for octaphenyltetraazaporphine, $H_2Pc^tBu_4$ for tetra(4-*tert*-butyl)pthalocyanine, etc.

Solvents

AcOH	acetic acid
DMF	dimethylformamide
DMSO	dimethylsulphoxide
EtOH	ethanol
HMPTA	hexamethylphosphotriamide
MeCN	acetonitrile
solv	molecule of solvent

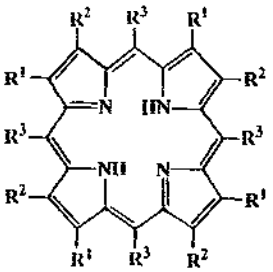

Porphyrins

$R^1=R^2=R^3=H$ -
porphine, H_2P

$R^1=R^2=H$; $R^3=Ph$ -
meso-tetraphenylporphine, H_2TPP

$R^1=R^2=H$; $R^3=Pr^n$ -
meso-tetra(n-propyl)porphine, H_2TPrP

$R^1=R^2=Et$; $R^3=H$ -
octaethylporphine, H_2OEP

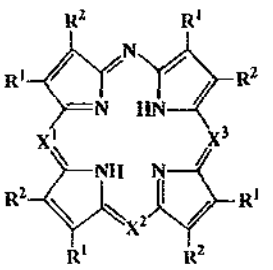

Azaporphyrins - H_2AP

$X^1=X^2-X^3=-CH=$ -
monoazaporphine, H_2MAP

$X^1=X^3=-CH=$; $X^2=-N=$ -
trans diazapophine, H_2DAP

$X^1=X^2=X^3=-N=$ -
tetraazaporphine, H_2TAP

in substituted derivatives
R^1 and/or R^2 are other than H -
$H_2MAP(R^1R^2)_4$, $H_2DAP(R^1R^2)_4$,
$H_2TAP(R^1R^2)_4$

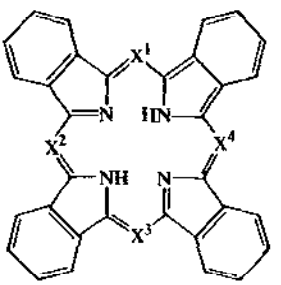

Tetrabenzoporphyrins

$X^1=X^2=X^3=X^4=-CH=$ -
tetrabenzoporphine, H_2TBP

$X^1=-N=$; $X^2-X^3=X^4=-CH=$ -
monoazatetrabenzoporphine, H_2MATBP

$X^1=X^2=X^3=-N=$; $X^4-CH=$ -
triazatetrabenzoporphine, H_2TATBP

$X^1=X^2=X^3=X^4=-N-$
phthalocyanine, H_2Pc

Other abbreviations

HS	hydrogen-bonded structure
IS	ionized structure
LS	localized (bonded) structure
US	unlocalized (shared or bridged) structure

1. Introduction

The most important property of porphyrins as ligands is their ability to react with metal salts with the formation of chelate complexes:

$$H_2P + MX_2 = MP + 2HX \quad (1)$$

The kinetics and mechanism of metal ion incorporation in porphyrin ligands have been the subject of intensive studies and their results have been reviewed [1–6]. However, these reviews, encompassing a great number of different porphyrins (both natural and synthetic) did not deal with the azaporphyrins nor with the related phthalocyanines (tetraazatetrabenzoporphyrins). Some of our studies of the coordination chemistry of tetraazaporphyrins were reviewed in a monograph [7] published in Russian. In this paper we discuss the influence of aza substitution on the structure of porphyrin ligands, on their coordination activity and on the peculiarities of the metalloazaporphyrin formation mechanism.

2. Structure of the reaction centre

The reaction centre of a porphyrin ligand (N_4H_2) is composed of four nitrogen atoms and two imino-hydrogen atoms of the pyrrole rings which participate directly in complex formation. The structure of the reaction centre, reflecting the geometry and electronic structure of the porphyrin molecule as a whole, has an important impact on the kinetic parameters of metalloporphyrin formation [4]. Its electronic structure dictates the state and stability of the N—H bonds and the solvation of the reaction centre. The dimensions of the coordination cavity determine the degree of steric compatibility between the ligand and the metal ion.

2.1. Geometry of the CN skeleton

X-ray crystallography is the most reliable method for the evaluation of the molecular geometry in the solid state. X-ray data have been reported for the free-base porphine (H_2P) [8,9] and some of its derivatives: *meso*-substituted tetraphenylporphine (H_2TPP) [10,11], tetrapropylporphine (H_2TPrP) [12] as well as β-substituted octaethylporphine (H_2OEP) [13]. Among azaporphyrins, only the structures of two tetrabenzoderivatives, namely monoazatetrabenzoporphine (H_2MATBP) [14] and tetrabenzotetraazaporphine commonly named phthalocyanine (H_2Pc) [15], have been studied by this method. The average structural data are represented in Table 1.

2.1.1. Porphyrins

The skeleton of common porphyrin ligands can be considered as almost planar since the deviations of the C and N atoms from the mean plane do not exceed 0.006 nm [8–13]. The symmetry of the skeleton is in most cases D_{2h} [9,11–13]. A D_{4h} skeletal symmetry was found for monoclinic H_2P [8] and tetragonal H_2TPP [10]. D_{2h} distortion of the porphyrin ligands is connected above all with the inequivalency of the five-membered rings composing the macrocycle. In two trans-located pyrrole type-rings (A) the bonds $C_\alpha—C_\beta$ are about 0.002–0.003 nm shorter, $C_\beta—C_\beta$ bonds are about 0.002 nm longer and the inner angle formed by the nitrogen atom is 2.5–4° larger compared with a pair of the neighbouring pyrrolenine-type rings (B). At the same time the bond lengths between C_α atoms and the inner nitrogen atoms vary only slightly in these two ring types and are 0.002–0.003 nm shorter than the

Table 1
Average geometrical parameters for the CN skeleton of porphyrin and azaporphyrin ligands

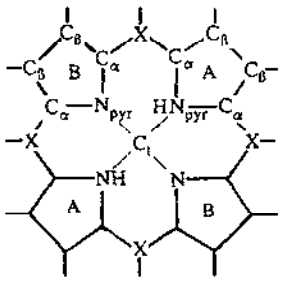

A - pyrrole-type ring

B - pyrrolenine-type ring

Geometric parameter	H_2P[a] [8]	H_2OEP[a] [13]	H_2TPP[a] [10]	H_2MATBP [14]	H_2Pc [15]	H_2Pc [16]	H_2TAP [34]
C_α–X (nm)	0.1376	0.1394	0.1400	0.125 (N)	0.1335	0.132	0.133
	0.1387	0.1390		0.139 (C)			
C_α–N_{pyr} (nm)	0.1377	0.1364	0.1364	0.145	0.1340	0.137	0.136
	0.1380	0.1367	0.1374				
C_α–C_β (nm)	0.1452	0.1462	0.1455	0.147	0.1490	0.147	0.144
	0.1431	0.1438	0.1428				
C_β–C_β (nm)	0.1345	0.1353	0.1347	0.152	0.1390	0.140	0.134
	0.1365	0.1373	0.1355				
N_{pyr}–C_t (nm)	0.2051	0.2062	0.2060		0.1913		0.194
C_α–X–C_α (°)	126.9	127.7	125.6	111 (N)	115	122	122
				143 (C)	119	125	
C_α–N_{pyr}–C_α (°)	106.1	105.7	106.2	109	109	109	108
	108.5	109.6	109.2				
X–C_α–N_{pyr} (°)	125.1	125.0	126.2	132 (N)	131	127	128
				123 (C)		130	

[a] Data are given for pyrrolenine- and pyrrole-type rings.

bonds of C_α atom with C_{meso} atom. The symmetric alkyl or aryl substitution in the *meso* or β positions has little influence; the changes in the bond lengths and values of the angles do not exceed 0.002 nm and 2°. The dimensions of the central coordination cavity (measured as a distance between the intracyclic N atoms N_{pyr} and the macrocycle centre C_t) vary slightly in the range 0.204–0.206 nm. One can expect that the direct substitution of the carbon atom in the conjugated π system of the porphyrin with a heteroatom, namely aza substitution in the *meso* positions, should

produce significantly greater changes in the geometry of the reaction centre and that is the case in fact.

2.1.2. Phthalocyanine

The only X-ray study of metal-free phthalocyanine made by Robertson [15] in 1936 showed that the H_2Pc molecule is planar and has D_{2h} symmetry. Unlike porphyrins this D_{2h} distortion of the tetragonal symmetry of the skeleton owes its origin not to the inequivalence of pyrrole rings but to the difference in the angles formed by neighbouring *meso*-nitrogen atoms (115 and 119°). The bonds composing the inner 16-membered macroring in H_2Pc are shorter than in the porphyrins. The bonds formed by the bridge atoms (in this case *meso*-nitrogen atoms) are considerably shortened. Thus the alternation of the bonds of the inner macrocycle which is noticeable in porphyrins (about 0.137 nm for $C_\alpha-N_{pyr}$ and 0.139–0.140 nm for $C_\alpha-C_{meso}$ bonds) is barely perceptible in phthalocyanine ($C_\alpha-N_{pyr}$, 0.134 nm; $C_\alpha-N_{meso}$, 0.133–0.134 nm). The values of the angles formed with participation of the bridge atoms also change. In comparison with porphyrins the angle $C_\alpha-X_{meso}-C_\alpha$ is decreased by 10° and the angle $N_{pyr}-C_\alpha-X_{meso}$ increased by 6°. These changes in bond lengths and angles lead to a significant shrinkage of the central coordination cavity, by 0.026 nm compared with porphyrins. The geometry data for H_2Pc obtained by Hoskins et al. [16] by a neutron diffraction method differ somewhat from the data of Robertson [15]. However, the observed change in the dimensions of the reaction centre as one goes from porphyrins to phthalocyanine is the same. To what can these changes be attributed: to the influence of aza substitution or rather to benzo substitution?

2.1.3. The influence of benzo and aza substitution

Unfortunately structural data on unsubstituted H_2TAP and H_2TBP ligands which could provide a direct answer to this question are lacking until now. Although preliminary X-ray studies on H_2TBP and its monoaza- and triaza-substituted derivatives made by Woodward [17] and Robertson [18] did not resolve the structures of these molecules; yet on a basis of the crystal parameters they supposed that the structure of the monoaza derivative (H_2MATBP) should be like the structure of H_2TBP and differ essentially from the structure of the triaza derivative (H_2TATBP) which should be more like the phthalocyanine. Later Das and Chandhuri [14] evaluated the structure of H_2MATBP and showed that monoaza substitution provokes a significant distortion of the molecule. The deviations from the mean plane reach 0.0311 nm. The bond lengths and bond angles formed by the *meso*-nitrogen atom (0.125 nm and 111°) are significantly less than formed by the *meso*-carbon atoms (average values of 0.139 nm and 143°). The inner angle formed by the bridge atom with the isoindole rings ($X_{meso}-C_\alpha-N_{pyr}$) is larger in the case of *meso*-nitrogen (132°) than of *meso*-carbon (123°). A similar but weaker effect of monoaza substitution on the geometry of the macrocycle was observed for the Fe complex of octaethylmonoazaporphine ($ClFeMAPEt_8$) [19].

Recently the results of the first X-ray investigations of complexes of tetraazaporphyrins were published [20,21]. Comparison of these structural data with the data on

corresponding complexes of porphyrins [22–24], tetrabenzoporphine [25] and phthalocyanine [26,27] reveal the separate influence of aza and benzo substitution. In order to reveal what structural changes are produced in the CN skeleton of the porphyrin ligand by tetrabenzo and tetraaza substitution we consider the available structural data on the metal-free compounds (H_2P, H_2OEP, H_2TPP and H_2Pc) and complexes of Fe (ClFePc [27], ClFeOETAP [21], ClFeTPP [23], and ClO_4FeOEP [22]) and Ni (NiPc [26], NiTBP [25] and NiTMP [24]). Fig. 1 displays changes in the geometry produced by tetrabenzo substitution in porphyrins and tetraazaporphyrins and by tetraaza substitution in porphyrins and tetrabenzoporphyrins. Aza substitution reduces the angles formed by a bridge atom and shortens the bonds composing the inner 16-membered ring. In the case of porphyrins the bond between C_α atom and *meso*-atom is especially shortened. Only the N_{pyr}—C_α bonds change significantly in the isoindole fragments, whereas in the pyrrole fragments the isolation of ethylene double bonds is distinct and their geometry changes drastically. Benzo substitution has little impact on the geometry of the inner macroring in tetraazaporphyrins, while in the porphyrins the bonds and angles formed by the bridge carbon atom are significantly reduced.

Thus the comparison of metallocomplex structures reveals that aza substitution affects the geometry more strongly than benzo substitution and that its effect is more pronounced in porphyrins (and their alkyl and aryl derivatives) than in tetra-

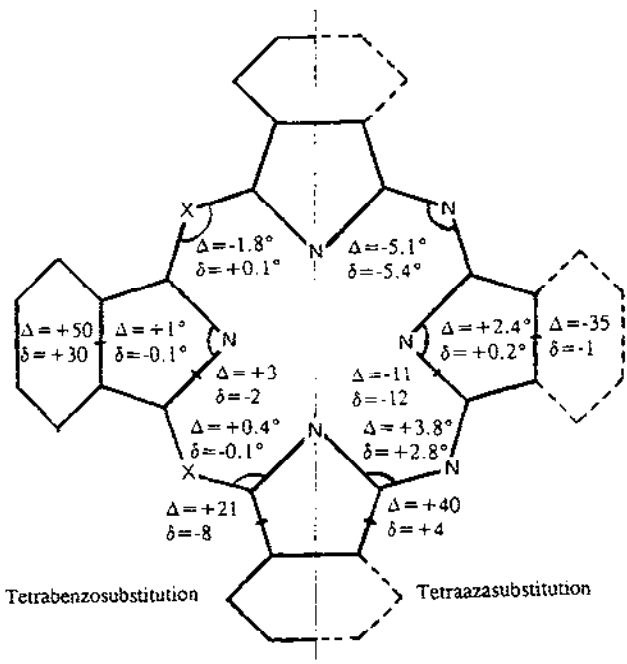

Fig. 1. Changes in the geometry of the CN skeleton produced by tetrabenzo substitution (left side) in porphyrins (Δ) and tetraazaporphyrins (δ) and by tetraaza substitution (right side) in porphyrins (Δ) and tetrabenzoporphyrins (δ). The angles are in degrees, and the bond lengths in 10^4 nm.

benzoporphyrins. One can expect that in the free ligands, in the absence of a central metal ion rigidly bonding the inner nitrogen atoms, the effect of aza substitution will be greater.

The influence of aza substitution in porphyrins on their electronic structure was intensively studied by quantum chemistry methods [28–30]. The most comprehensive review of this area was published by Solovyov and co-workers [31]. Calculations of the H_2TAP molecule were based on the geometry of H_2P [28,31], H_2Pc [29,32,33] or an idealized geometry [30]. They all show poor consistency with experimental data (for example with UV–visible spectra) than in the case of H_2P or H_2Pc, where the experimental geometry based on X-ray data were available. No successful optimization of the H_2TAP skeleton geometry was made in these studies to achieve better consistency. On the basis of X-ray structural data for porphyrines, tetrabenzoporphine and its monoaza-, triaza- and tetraaza-substituted derivatives in Ref. [34] empirical structural parameters for H_2TAP were suggested. They are presented in Table 1 in regard to the recent data on tetraazaporphyrin metal complexes [20,21].

2.2. *The location of the NH hydrogen atoms and the state of the N—H bonds*

The following possible structures for the N_4H_2 centre in porphyrin-like ligands are usually debated (Fig. 2): LS, localized (bonded) structure in which the H atoms are located on the line combining the opposite N atoms of the pyrrole rings and bonded with them with two-centre covalent bonds; US, unlocalized structure (known also as shared or bridged) in which the H atoms form three-centre bonds with two N atoms of adjacent pyrrole rings and are located on the line combining the opposite *meso* atoms; HS, hydrogen-bonded structure which is intermediate between LS and US (each H atom forms a mostly covalent bond with one N atom and a strong H bond with the neighbouring N atom); IS, ionized structure in which two protons are located in the field of the ligand dianion (Fig. 2). One can see that in the LS and HS structures the internal nitrogen atoms are inequivalent: two atoms of aza (pyridine) type and two of imino (pyrrole) type. In the US and IS structures all four internal nitrogen atoms are equivalent.

X-ray data defining the atoms of the CN skeleton are not sufficiently reliable in the case of hydrogen atoms. Neutron diffraction can give more reliable data about the H atom positions. However, it is well to bear in mind that these methods can reveal only the static structure of the molecule in the solid state which can differ significantly from the structure in the vapour phase and especially in solution. Thus the N_4H_2 centre structure must be resolved by a combination of diffraction methods, spectroscopic methods and quantum chemistry methods. The acid–base properties also provide important information about their structure in solution (see below).

2.2.1. *Porphyrins*

According to X-ray studies of common porphyrin ligands, two internal H atoms are most probably localized near the line connecting two opposite N atoms [8,9,11–13] or are equally distributed between all four nitrogen atoms (each bears half a hydrogen atom) as in the case of tetragonal H_2TPP [10] with an N—H

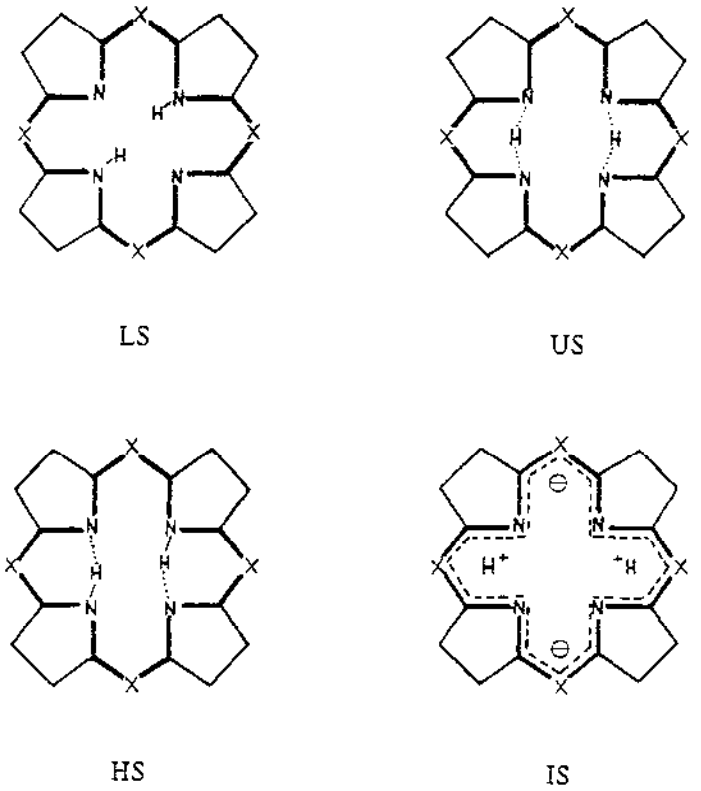

Fig. 2. The possible structures of the N_4H_2 reaction centre in porphyrin-type ligands, where X ≡ CH in porphyrins, X ≡ N in azaporphyrins: LS, localized (bonded) structure; US, unlocalized (shared or bridged structure); HS, hydrogen-bonded structure; IS, intraionized structure.

distance of 0.092–0.096 nm. The X-ray photoelectron spectra of H_2TPP [35] and benzo-substituted porphyrins [36] shows the existence of two types of nitrogen atom with different N 1s binding energies, which is also consistent with the LS structure. Schaffer and Gouterman [29] used the EHMO method to investigate the location of the inner protons in porphine and found better agreement with the experimental UV–visible spectrum for the LS than for the US structure. IR spectroscopy data give evidence of intramolecular H bonds [37–39]. The complete neglect of differential overlap 2 (CNDO/2) calculations [40,41] also substantiate the tendency for H bonding in porphyrins which can be achieved without displacement of H atoms from the line connecting the opposite nitrogen atoms when each of the H atoms forms two equivalent H bonds with both of the neighbouring aza atoms.

The static model is not adequate to describe the reaction centre. Early studies of the PMR spectra of porphyrins [42] showed the existence of fast NH tautomery (the lifetime of each tautomer at ambient temperature is not more than 0.02 s) which can be inhibited only at low temperatures. Different dynamic models for the N_4H_2 centre structure in porphyrins and mechanisms of NH tautomery were suggested on

the basis of ^{1}H, ^{13}C, and ^{15}N nuclear magnetic resonance (NMR) spectroscopy and on quantum-chemical calculations and were reviewed by Mamaev et al. [43] in 1989. The porphyrin reaction centre can be conceived as two tautomeric LS structures. Weak intramolecular H bonding of the H atoms with both aza atoms promotes tautomery which proceeds according to the asynchronous tunnel mechanism at 150–300 K and according to the synchronous mechanism at lower temperatures [43]. Such a structure is also in agreement with the behaviour of porphyrin ligands in complex formation reactions and with their acid–base properties [6].

2.2.2. Phthalocyanine and azaporphyrins

Neither Das and Chandhuri (for H_2MATBP [14]) nor Robertson (for H_2Pc [15]) speculated about the position of the internal hydrogen atoms on the basis of their X-ray data.

Berezin [44,45], using the X-ray data of Robertson [15] and his own investigation of the behaviour of H_2Pc and its complexes in acid media, suggested the inner ionized IS-type structure "which explains practically all physicochemical properties of phthalocyanine in solution" [6, p. 50]. Later Fleischer [46] reanalysed the X-ray data of Robertson and proposed the bridged US-type structure for H_2Pc. In a neutron diffraction study made by Hoskins et al. [16] the two internal hydrogen atoms "appeared as ... four half-hydrogen atoms, one associated with each of pyrrole nitrogen atoms ... with an average distance 0.094 nm". As with tetragonal H_2TPP [10] this result favoured the LS structure.

Apart from these data, only IR and UV-visible data were available for H_2Pc and H_2TAP for a long time. The observed shift in the ν_{NH} frequencies in the IR spectra of the solid samples in the order H_2P (3305 cm^{-1}) > H_2TAP (3300 cm^{-1}) > H_2Pc (3290 cm^{-1}) was considered by Berezin [4, p. 57] as evidence of N—H bond polarization. However, it is indicative rather of the strengthening of intramolecular H bonding, i.e. of the HS or US structures than of the IS structure. Sharp and Lardon [47] explained the observed red shift in the ν_{NH} frequency in β-H_2Pc (3284 cm^{-1}) compared with α-H_2Pc (3302 cm^{-1}) as a result of the intermolecular H bonding in the β form.

The positions of the long-wave band Q_x and especially the splittings $\Delta E(Q)$ of the Q band in the UV–visible spectra of H_2Pc differ significantly in the vapour (Q_x = 14 580; $\Delta E(Q)$ = 1490 cm^{-1} [48]), in solution (1-chloronaphthalene): (Q_x = 14 327; $\Delta E(Q)$ = 733 cm^{-1} [49]) and in different modifications of the solid state (α-H_2Pc; Q_x = 14 510; $\Delta E(Q)$ = 1200 cm^{-1}) (β-H_2Pc; Q_x = 13 970; $\Delta E(Q)$ = 1530 cm^{-1} [50]). Solovyov [51] suggested that such distinctions in $\Delta E(Q)$ are connected with the different molecular structures of H_2Pc in the vapour, in solution and in the solid state.

2.2.2.1. Quantum-chemical investigations. UV–visible [47–50] and structural [15,16] data provided the experimental basis for numerous efforts to solve the problem using quantum-chemical methods [29,32,52,53]. Usually the agreement between the experimental UV–visible spectra and the calculated spectra was used as a criterion of goodness of the implied model. The simple Hückel calculation of H_2Pc made by Chen [52] provided support for the US structure. Orti et al. [32] have calculated

the UV–visible spectrum of H_2Pc assuming the LS model on the basis of the geometry employed by Hoskins et al. [16] and using a valence effective hamiltonian non-empirical pseudopotential method. The results were in good agreement for $\Delta E(Q)$ only for the vapour spectra of H_2Pc but the energy of the Q_x transition was greatly underestimated. Berkowitch-Yellin and Ellis [33] used a one-electron Hartree–Fock–Slater model in their calculations and supported the US structure for H_2Pc. The most comprehensive studies of the influence of the CN skeletal structure on the location of the internal hydrogen atoms in H_2Pc were made in Refs. [29,53].

Schaffer and Gouterman [29] used the extended Hückel method and found that the bonded model with the D_{4h} skeleton (LS structure) gives a calculated energy gap between Q_x and Q_y transitions ($\Delta E(Q) = 1440\ cm^{-1}$) which is very close to the experimental value of the H_2Pc spectrum in the vapour ($1490\ cm^{-1}$) or in the solid ($1530\ cm^{-1}$). However, the splitting parameter of the solution spectrum ($\Delta E(Q) = 730\ cm^{-1}$) could not be achieved for the bonded model and was obtained only on the basis of the bridge (US) model with significant distortion of the CN skeleton. In all cases the calculations [29] gave a lower energy for the Q_x transitions ($12\,300$–$13\,300\ cm^{-1}$) than experimental values. Schaffer and Gouterman also concluded that the structure of H_2Pc depends strongly on environment and can differ in vapour, in solid state and in solution.

Mamaev et al. [53] investigated the structure of the H_2Pc reaction centre with CNDO/S using dynamic models. As in Ref. [29] the experimental geometry of the CN skeleton [15] was preferable for the LS structure which is about 120 kJ mol^{-1} more stable than the US structure. The spectrum observed in solution was well reproduced (calculated; $Q_x = 14026$; $\Delta E(Q) = 711\ cm^{-1}$) when the $N_{meso}-C_\alpha-N_{pyr}$ angle was reduced from the experimental value in the solid state (131° [15]) to 127° and all other parameters remained unchanged. The location of the internal hydrogen atoms has only a small effect on the Q band splitting (608 and 711 cm^{-1} for LS and US structures respectively) but greatly influences the splitting of the B band located in the UV region. This splitting is predicted to be two and a half times larger for the LS structure (1613 and $632\ cm^{-1}$ for the LS and US structures respectively). Since for this distorted skeleton the total energy for the US structure was calculated to be 50 kJ mol^{-1} less than for the LS structure and no splitting (only broadening) is observed for the B band in the experimental solution spectrum, the US model is favoured for solution. Mamaev et al. [53] concluded that the transition from the solid state to the solution causes deformation of the CN skeleton and the structure of H_2Pc changes from LS to US which is about 80 kJ mol^{-1} more stable. However, since the energy difference between the LS and US structures is not large, small changes in the intermolecular interactions can lead to distortion of the H_2Pc geometry and to the transition from one structure to another. On the basis of the dynamic model of the reaction centre the adiabatic potential surface for the synchronous movement of protons in the reaction centre was calculated [53]. For the LS structure, this surface has four potential wells with barriers of 120 and 230 kJ mol^{-1} which is less than for H_2TAP (300 kJ mol^{-1} [54]) and for H_2P (394 kJ mol^{-1} [43]). For the US structure the surface has only two potential wells with a barrier of 660 kJ mol^{-1}.

Theoretical consideration of the H_2TAP reaction centre has received less attention.

Table 2
UV–visible spectra of H_2TAP: experimental and calculated parameters

Conditions	Reference	Structure of reaction centre	Energy of electronic transitions (cm^{-1})				Splitting (cm^{-1})	
			Q_x	Q_y	B_x	B_y	ΔQ	ΔB
Experimental								
In KBr at 10 K			16155	18210	30210sh	32470	2055	2260
In EtOH			16320	18500	30120	31350sh	2180	1230
In AcOH			16290	18440	30160	31550sh	2150	1390
In pyridine			16220	18290	29605	30170sh	2070	565
Calculated								
	[33]	US	16800	19100			2300	
	[33]	LS	15500	20600			5100	
	[29]	US	11510	13032			1522	
	[29]	LS	12740	14190			1110	
	[32]	LS	12324	13864			1450	

Schaffer and Gouterman [29] calculated the spectrum of H_2TAP but neither a bonded nor a bridged model gave results comparable with experimental spectroscopic values of Q_x and $\Delta E(Q)$ (Table 2). Orti et al. [32] used the LS model and their results also show poor agreement. The theoretical UV–visible spectrum of H_2TAP obtained by Berkowitch-Yellin and Ellis [33] gave good agreement in the case of the US structure. Since all these calculations were based on the H_2Pc geometry, they should be considered with caution.

Consider next how these theoretical observations agree with experimental results of other spectroscopic methods (X-ray photoelectron spectroscopy (PES) and NMR) and with data recently obtained on the acidity constants of porphyrins, azaporphyrins and phthalocyanine.

2.2.2.2. X-ray photoelectron spectroscopy. X-ray photoelectron spectra were reported for H_2TPP [35], for benzoporphyrins [36] and for their monoaza-, triaza- and tetraaza-substituted derivatives [35,55,56] (Table 3). When one proceeds from H_2TPP [35] or benzo-substituted porphyrin (tribenzo(1-phenyl-2,3-naphthalo)porphine (H_2NTBP) [36]) to H_2Pc the low energy N 1s peak (about 397.7–398.9 eV) corresponding to the aza-nitrogen increases its intensity in comparison with the high energy peak of the imino-nitrogen atoms (399.6–400.4 eV) proportional to the number of nitrogen atoms introduced in the *meso* position which are also of aza type. This does not correspond to the US or IS structures where all internal nitrogen atoms are equivalent and Niwa et al. [35,55] came to the conclusion of an LS structure without H bonding. This conclusion seems inappropriate. Since it is generally known that aza substitution reduces the basicity of aromatic heterocycles and that H_2Pc has more distinct aromatic character and is a much weaker base than H_2TPP or H_2TBP [4,6], the shift of all 1s binding energy peaks to higher

Table 3
1 s binding energies for atoms of the CN skeleton in porphyrin-type ligands

Compound	Binding energy (eV)				Relative intensity I_{imino}/I_{aza}	Reference
	C 1s	N 1s				
		"Aza"	"Imino"	ΔE(N 1s)		
H_2TPP	284.8	398.2	400.2	2.0	1.12	[35]
H_2NTBP		397.2	399.6	2.4	≈1	[36]
H_2MATBP		398.3	400.1	1.8	0.78	[55]
H_2TATBP		398.9	400.5	1.6	0.52	[55]
H_2Pc	286.2	398.9	400.4	1.5	0.40	[35]
		397.9 (broad)				[56]
$E(H_2NTBP)$-$E(H_2Pc)$	−1.4	−1.7	−0.8	−0.5		

energies as a result of aza substitution in tetrabenzoporphyrins is not surprising. However, at the same time the high energy shift of the imino-nitrogen peak is about half that of the aza-nitrogen (internal or *meso*) or for carbon atoms of the pyrrole rings and the energy difference between the N 1s peaks of the "imino" and "aza" nitrogen atoms is reduced from 2.4 eV for H_2NTBP to 1.5 eV for H_2Pc. Bearing this in mind and using the thesis of Niwa et al. [55] that "when the N−H bond of the pyrrole is elongated by a hydrogen bonding interaction ... the 1s binding energy of the pyrrole nitrogen atoms should become lower than otherwise" one comes to the conclusion that aza substitution leads to strengthening of the H bonding in the reaction centre, i.e. to an HS structure in the solid state. The H-bonding interaction with the "aza" nitrogen atoms results, in this case, in a more distinct shift in their N 1s binding energy peak to higher energy than the C 1s peak of the carbon atoms. It is interesting to note that Zeller and Hayes [56] observed only one broad peak centred at 397.9 eV with their sample of H_2Pc.

2.2.2.3. Nuclear magnetic resonance spectroscopy in the solid state. Solid samples of H_2Pc were also investigated by ^{1}H [57], ^{13}C [58] and ^{15}N [59] NMR spectroscopy.

Dudreva and Grande [57] measured the dependence of the spin–lattice relaxation time in the temperature range from −140 to +150 °C for different crystallic modifications of H_2Pc (α, β and γ) and for D_2Pc using the PMR method. They came to a conclusion about intramolecular H bonds and about intramolecular proton exchange at low temperatures and supposed the diffusion of protons among the molecules of solid substance above room temperature. The potential barrier was estimated as 28 kJ mol^{-1}.

Meyer et al. [58] using ^{13}C NMR spectroscopy observed the tautomery process for α-H_2Pc and determined the rate of proton exchange which appears to be higher than for solid H_2P [60] (k_{HH} = 5200 and 1620 s^{-1} respectively at 260 K). The data presented allow one to estimate roughly the activation energy to be 33 kJ mol^{-1}. It was concluded [58] that the existence of two types of C_α and C_β atom provides

evidence for two inequivalent isoindole fragments and therefore for the LS structure. We should like to mention that in the HS as well as in the US and IS structures there are also two pairs of inequivalent C_α and C_β atoms in each isoindole fragment and two tautomeric forms are also possible.

Kendrick et al. [59] reported ^{15}N NMR spectra for H_2Pc. The spectral changes observed with temperature were interpreted as double-proton transfer in the LS structure which is fast on the NMR time scale at 300 K and slow at 153 K just as it is in solid H_2P [60]. Such an interpretation seems inappropriate for H_2Pc. As one can see (Fig. 3) in the LS structure of H_2Pc there are three types of nitrogen: two imino-nitrogen atoms, two internal aza-nitrogen atoms and four *meso*-nitrogen atoms which are also of the aza type. *Meso*-nitrogen atoms in the LS structure of H_2Pc are equivalent, do not take part in proton exchange and should give a singlet at any temperature. Internal aza- and imino-nitrogen atoms in the LS structure should give two signals at low temperatures and one broadened signal at high temperatures when the exchange process is fast. Such behaviour was observed for H_2P [60] when the doublet for imino- and aza-nitrogen atoms at 192 K (107 and 215 ppm respectively) coalesces without combination of the doublet peaks into a broad singlet at 161 ppm, at ambient temperature. This singlet becomes sharp at higher temperatures. In the spectrum of H_2Pc at 153 K the signal at 195 ppm corresponds to the four *meso*-nitrogen atoms, the shoulder at 191 ppm to two internal aza-nitrogen atoms and the singlet at 104 ppm to two imino-nitrogen atoms as might be expected for a localized structure with a slow exchange rate. However, at 300 K, contrary to expectation for the LS structure, two sharp singlets are not observed bur rather two doublets: the first at 141 and 160 ppm and the second at 190 and 194 ppm. Such a view of the spectrum corresponds best to the HS structure for H_2Pc with a slow exchange rate. In this structure the *meso*-nitrogen atoms are inequivalent; one pair, which are due to the weak interaction with the internal hydrogen atoms, resonate slightly more upfield (190 ppm) than the other pair (194 ppm). Two pairs of internal nitrogen atoms also differ; the signal of two aza-nitrogen atoms shifts upfield to 161 ppm owing to the strong H bonding compared with the LS structure (191 ppm) and the signal of two imino-nitrogen atoms shifts downfield to 141 ppm (104 ppm in the LS structure) owing to the weakening of NH bonds. With increasing temperature the LS structure of H_2Pc transforms to the more stable HS structure. Proton exchange in the HS structure is also slow on the NMR time scale at 300 K. This interpretation is also consistent with the above mentioned calculations of Mamaev et al. [53] who showed that proton transfer processes for the delocalized structure of H_2Pc should proceed through a double-minimum potential with an activation energy three times higher than for the LS structure with a four-minimum potential.

2.2.2.4. Nuclear magnetic resonance spectroscopy in solution. The PMR spectrum of the unsubstituted H_2Pc was obtained [61] only in the D_2SO_4 solution because of its poor solubility in organic solvents. No signal of the internal NH protons was observed but only multiplets of the benzene-ring CH protons (9.59 and 8.52 ppm) which appeared to be similar to spectra of the metal complexes. In the last few decades, many substituted metal-free phthalocyanine derivatives have become avail-

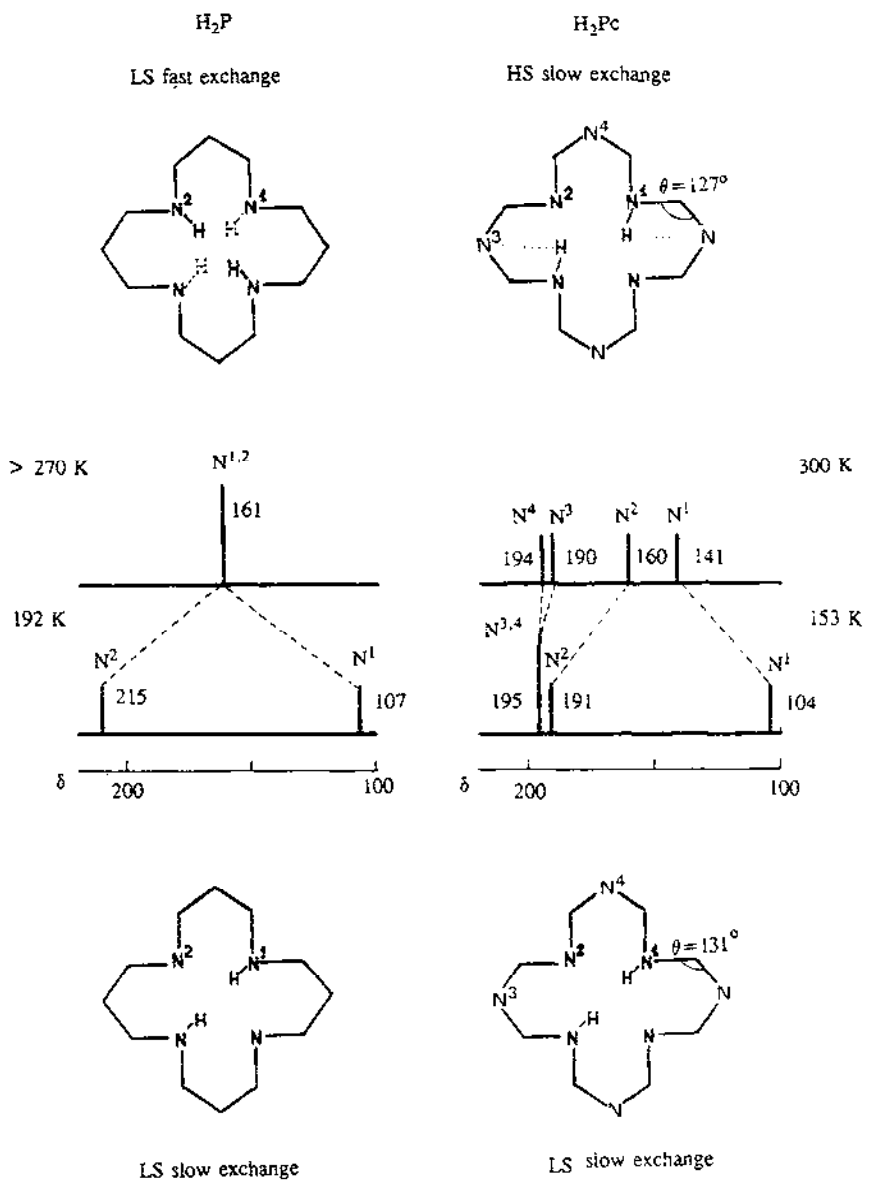

Fig. 3. Interpretation of the ^{15}N NMR spectra of solid H_2P and H_2Pc. Values of the chemical shifts are from [59] for H_2Pc and from [60] for H_2P.

able [62]. The introduction of alkyl and alkyl-containing groups in the benzene rings endows the phthalocyanine molecule with higher solubility in organic solvents. Some such derivatives were characterized by the PMR spectroscopy method ([63,64]; see also the review in [62] and references therein).

Andronova and Luk'yanets [63] first reported the PMR spectrum of the soluble

substituted derivative, tetra (4-*tert*-butyl)phthalocyanine ($H_2Pc^tBu_4$). They observed a broad peak of the internal NH protons in the strong field (−5.3 ppm) in CCl_4 solution at room temperature, together with the signal of the *tert*-butyl group protons (1.72 ppm) and the multiplet of the benzene rings protons (7.5–8.4 ppm) Later Hanack et al. [64] reported the PMR spectrum of $H_2Pc^tBu_4$ in $CDCl_3$. Although the chemical shifts of the benzene and *tert*-butyl protons have similar values as in [63], the NH-proton singlet was observed at −2.0 ppm. The reason for such a large difference in the chemical shift of the NH protons reported in these studies became clear when Leznoff and co-workers [65] investigated the PMR spectra of the monomeric and dimeric alkyloxy derivatives of phthalocyanine and found that aggregation had a great impact on the NH-proton signal, resulting in its upfield shift. With a solution of tetra(4-*neo*-pentoxy)phthalocyanine ($H_2Pc(OCH_2{}^tBu)_4$) in $CDCl_3$ the signal shifts from −5.5 ppm at 10^{-1} M to −3.0 ppm at 10^{-3} M and does not change upon further dilution. The 10^{-4}–10^{-3} M solutions most probably represent free non-aggregated phthalocyanines at room and even at lower (down to −80 °C) temperatures [65]. Although the $H_2Pc^tBu_4$ concentrations in the solutions investigated were not reported, one can suppose that Andronova and Luk'yanets [63] using an 80 MHz spectrometer obtained the spectrum of the aggregated form whereas Hanack et al. [64] using a more modern 360 MHz spectrometer were able to study a dilute solution containing the non-aggregated compound.

Experimental data show that aza substitution in the tetrabenzoporphyrin molecule induces considerable deshielding of the internal protons and their resonance is shifted downfield from −4.13 ppm for $H_2TBP^tBu_4$ [68] to −2.0 ppm for $H_2Pc^tBu_4$ [64]. Borovkov and Akopov [67] investigated the triaza derivative ($H_2TATBP^tBu_4$) and observed resonance of the internal protons as a multiplet in the range between −2.5 and −3.2 ppm at room temperature. Vysotsky et al. [68] using the molecular orbital self-consistent atomic orbital self-consistent field method and supposing the LS structure of the reaction centre, calculated NMR shifts for porphyrins and their aza and benzo derivatives and predicted a much smaller effect of aza substitution. The calculated value of the NH-proton resonance of H_2Pc ($\delta_{NH} = -3.37$ ppm) is shifted downfield only slightly compared with H_2TBP ($\delta_{NH} = -3.76$ ppm). These calculations give good agreement with experimental values of the NH-proton shifts for porphyrins where the bonded LS structure of the reaction centre is the case (H_2P; calculated, −3.82 ppm; experimental, −3.94 ppm [42c]); (H_2TBP; calculated, −3.76 ppm; experimental, −4.13 ppm (for $H_2TBP^tBu_4$) [66]), whereas for H_2Pc the calculated value ($\delta_{NH} = -3.37$ ppm) is lower than experimentally observed even for derivatives with substituents having a strong shielding effect ($H_2Pc(SiMe_3)_4$, $\delta_{NH} = -2.7$ ppm [64]). When it is taken in account that the higher aromaticity of the phthalocyanine molecule when compared with porphyrins should induce an upfield shift of the internal proton signal, the observed downfield shift can better be explained on the basis of the delocalized US and HS structures in which the shielding influence of the π-electron ring current of the aromatic macrocycle on the internal protons is compensated by the stronger polarization of the N—H bonds. The high acidity of the N—H bonds leads to a rapid exchange of the internal protons with the medium; the

NH-proton peak disappears when D_2O is added to the CCl_4 solution of the $H_2Pc^tBu_4$ [63], and no NH-proton signal is observed in the PMR spectrum of H_2Pc in D_2SO_4 [61].

Borovkov and Akopov [67] studied the temperature dependence of the PMR spectra of triazatetra(4-*tert*-butylbenzo)porphine ($H_2TATBP^tBu_4$) and concluded that, at ambient temperatures, $H_2TATBP^tBu_4$ exists in CS_2 as a mixture of two US structures, an asymmetric structure and a symmetric structure as follows:

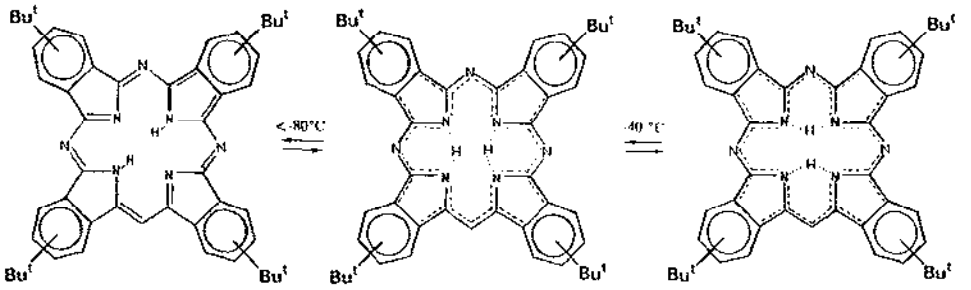

Lowering of the temperature to −40 °C shifts the equilibrium to the symmetric US structure. Further reduction in the temperature leads to conversion of the symmetrical US structure to the LS structure which has lower symmetry and was also supposed by Niwa et al. [55] for solid H_2TATBP on the basis of X-ray PES measurements. The solvent also influences the equilibrium of the two US forms. Replacement of CS_2 by solvents with better solvation abilities (pyridine) shifts the equilibrium to the symmetric US structure. Connecting the influence of solvent and temperature on the NH-resonance form with the structure of the reaction centre, Borokov and Akopov [67], however, did not take into account that the same factors also have an impact on the extent of aggregation [65] which may be reflected in similar changes of the NH absorbance.

Kopranenkov and coworkers [69] reported the PMR spectra of tetra(*tert*-butyl)-tetraazaporphine ($H_2TAP^tBu_4$) and for its randomers. At ambient temperature the β-CH proton singlet was observed at about 8.90 ppm and the NH-proton signal in the range −2.45–−2.59 ppm depending on solvent. Lowering of the temperature causes a downfield shift in the NH protons to −2.87 ppm (−88 °C). At the same time the β-CH proton singlet splits into two signals owing to NH tautomery (8.69 and 9.08 ppm) with a coalescence temperature of −69 °C. The value determined for $\Delta G^{\neq}$ of 41.4 kJ mol^{-1} is less than for porphyrins (H_2TPP, $\Delta G^{\neq} = 47.7$ kJ mol^{-1} [42d]) but higher than for H_2Pc in the solid (28–33 kJ mol^{-1} [57,58]). The same order of potential barriers was predicted by Mamaev and coworkers [43,53,54].

PMR spectra of the unsubstituted H_2TAP were obtained by Stuzhin [34]. In pyridine the β-CH proton singlet (9.24 ppm) is located at higher field than in H_2P (9.53 ppm [42c]). This upfield shift is not due to loss of aromaticity but can be explained by the larger isolation of the ethylene double bonds from the main 16-membered conjugation contour in which the π-electron ring current is stronger

than porphine [68]. This is also substantiated by the ^{13}C NMR spectroscopy data which have shown a downfield shift for the C_α signal and an upfield shift for the C_β signal for $H_2TAP^tBu_4$ [70] compared with porphyrins [42d]. The singlet of the internal NH protons in H_2TAP is observed at −0.97 ppm and is located in a substantially weaker field than for H_2P (−3.94 ppm [42c]). In as much as the higher aromaticity of H_2TAP [28–30,68] and the smaller diameter of its central cavity compared with H_2P should lead to the opposite upfield shift of the internal proton signal, this strong downfield shift is explained by changes in the state of the N−H bonds themselves. The polarization of the N−H bonds and the increase in the positive charge on the internal hydrogen atoms in H_2TAP reduces their shielding by the π-electron ring current and this manifests itself as a downfield shift. The state of the N−H bond is very sensitive to substituents in the pyrrole rings. Electron donors such as butyl or ethyl groups reduce the ionic character of the N−H bonds and cause an upfield shift of the NH-proton signal to between −2.1 and −2.6 ppm [69,71]; Br atoms as electron-acceptors increase the ionic character of the N−H bonds and the signal shifts downfield to +1.43 ppm [72].

The NH-proton resonance in H_2TAP and in its substituted derivatives is observed at a substantially lower field than was predicted by Vysotsky et al. [68] for the LS bonded structure ($\delta_{NH} = -4.62$ ppm). Therefore the delocalized US or HS structure of the reaction centre is favoured for H_2TAP in solution as well as for H_2Pc. Such a structure of the reaction centre with a high degree of ionization of the N−H bonds is also supported by direct measurement of the acid properties of porphyrins, phthalocyanine and tetraazaporphyrins [73–75].

2.2.3. *Acid ionization of porphyrins and tetraazaporphyrins in solution*

Porphyrin-type ligands can undergo two acid ionisation stages:

$$H_2P \rightleftharpoons H^+ + HP^- \quad (2)$$

$$HP^- \rightleftharpoons H^+ + P^{2-} \quad (3)$$

Acidity constants K_1 and K_2 characterizing these two stages for porphyrins and H_2TAP in DMSO were determined by Sheinin et al. [73–75]. Unlike common porphyrins (H_2P, H_2TPP and H_2TBP) which form only monoanions during the titration of their DMSO solution with $(NBu_4)^+OH^-$, both stage (2) and stage (3) take place in these conditions for H_2TAP. H_2TAP has an acidity ten orders of magnitude stronger than H_2P (pK_1 values in DMSO are 12.36 and 22.35 respectively) and therefore greater ionic character in the N−H bonds. In order to explain such a large difference in acidity the IS structure for H_2TAP (as previously also for H_2Pc [44,45]) was suggested, unlike H_2P for which the LS structure with weaker H bonds was substantiated [74,75]. Recently the acidity of H_2TAPBr_4 was also determined ($pK_1 = 7.26$ [76]).

Fig. 4 demonstrates the correlation between chemical shifts of the NH-proton resonances and constants of the first ionization stage (2) (pK_1) for porphyrins and

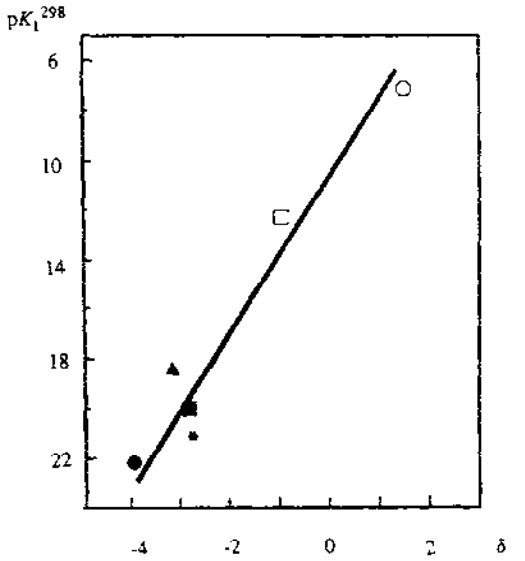

Fig. 4. The correlation between the NH-proton chemical shift δ_{NH} and acidity constants $pK_1^{298\ K}$ in DMSO for porphyrins ●, H_2P; ▲, H_2TBP; *, H_2TPP; ■, $H_2TPP(o\text{-}Cl)_4$ and tetraazaporphyrins (□, H_2TAP; ○, H_2TAPBr_4).

tetraazaporphyrins. The large dependence of the chemical shifts of the NH protons and of the acidity constants on the substituents in tetraazaporphyrins shows that the fully ionized structure IS is too idealized. It seems more probable that the bonding electrons are shared between three atoms forming the asymmetric H bond $N^{\delta'}-H^{\delta+}\cdots N^{\delta''-}$ or the symmetrical three centre bond $N^{\delta-}\cdots H^{2\delta+}\cdots N^{\delta-}$ (structures HS or US). In general the internal hydrogen atoms have distinct but only partial positive charge. For the US structure of H_2Pc this charge was calculated to be equal to +0.25 [53].

The N−H bond state in porphyrins and tetraazaporphyrins is determined by intramolecular interactions with substituents, by intermolecular interactions with neighbouring molecules in the solid state and by solvation in solutions. In porphyrins with a larger size of the coordination cavity, the LS structure with weak symmetric H bonds exists. In azaporphyrins and phthalocyanines where the conditions for strong H bonding are better owing to the smaller diameter of the coordination centre and electron-acceptor effect of the *meso*-nitrogen atoms, the HS and US structures can become favourable. According to V'yugin and co-workers [77], appreciable solvation of N−H groups in porphyrins is absent. Studies of tetraazaporphyrin solubility led Trofimenko and Berezin [78] to conclude the existence of specific solvation of N−H bonds in tetraazaporphyrins. Such solvation of the reaction centre is stronger for H_2TAP than for its alkyl-substituted derivatives having more covalent N−H bonds. The solvation has a strong influence on the state of the reaction centre in azaporphyrins and this also manifests itself in complex formation reactions.

3. Reactions of azaporphyrins with metal salts

3.1. General considerations

3.1.1. Metal incorporation–interaction with internal nitrogen atoms

In common with the porphyrins, the azaporphyrin ligands (H_2AP) react with metal salts yielding chelate complexes MAP according to the following general equation:

$$H_2AP + [MX_2(solv)_{n-2}] \rightarrow (solv)_m MAP + 2HX + (n-2-m)solv \quad (4)$$

where H_2AP is the azaporphyrin ligand, solv is the molecule of the solvent, MAP is the metalloazaporphyrin and $[MX_2(solv)_{n-2}]$ is the solvatocomplex of the metal salt.

Depending on the metal, the solvent molecules may remain bonded with the central metal atom in the azaporphyrin complex as extra ligands.

The reaction usually proceeds in a large excess of the metal salt, i.e. in pseudo-first-order conditions and therefore the kinetic equation for complex formation can be put into the form

$$\frac{-d[H_2AP]}{dt} = k_{eff}[H_2AP] \quad (5)$$

where the observed effective constant k_{eff} can depend on the metal salt concentration:

$$k_{eff} = k_v [M(OAc)_2]^n \quad (6)$$

The true constant k_v is independent of metal salt concentration. If the order n in the metal salt equals 1, reaction (4) obeys the bimolecular rate law; if $n=0$, it obeys the monomolecular rate law.

Since the rates of metal incorporation in porphyrin-like ligands are usually several orders of magnitude slower than the formation rates of complexes with simple ligands, they can be measured by conventional kinetic methods. The substantial difference between the UV–visible spectra of H_2AP and MAP and their high molar extinction coefficients make spectrophotometric methods especially convenient. Fig. 5 displays changes in the UV–visible spectra of H_2TAP in the presence of $Zn(OAc)_2$ in pyridine.

Complex formation reactions with common porphyrin ligands in organic solvents is first order both in porphyrin and in the metal salt [2,3,4, p. 80] and the bimolecular $S_{NE}2$ mechanism was established by Berezin [79]:

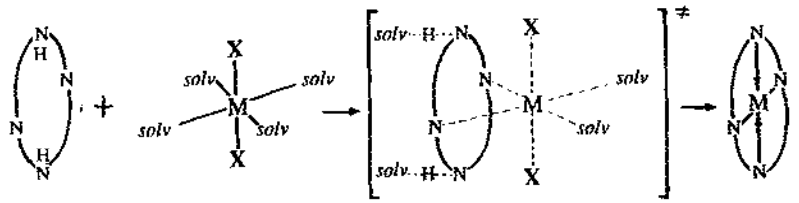

(7)

In accordance with this mechanism, the strength of the M—solv bonds ruptured during the activation stage has a very great impact on the kinetic parameters. The influence of the state of the N—H bonds which are only elongated in the transition

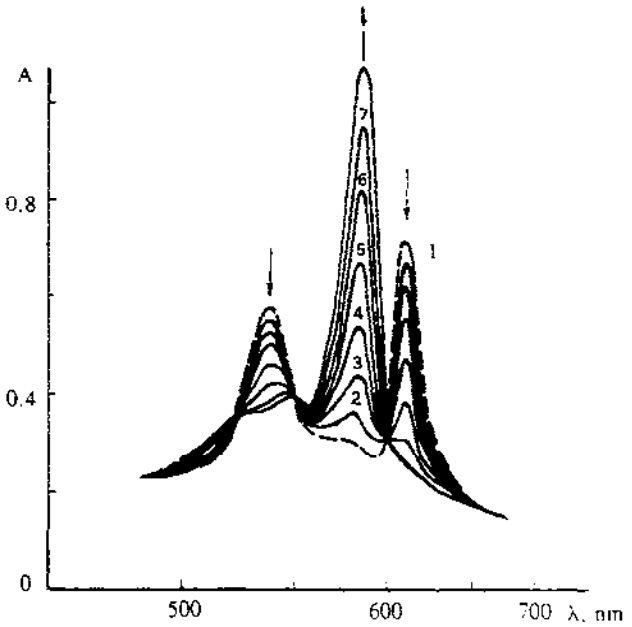

Fig. 5. UV–visible spectrum of the pyridine solution of H_2TAP (4.3×10^{-6} M) (spectrum 1) and its friction after the addition of $Zn(OAc)_2$ (2.5×10^{-4} M) at 298 K. Spectra 2, 3, 4, 5, 6 and 7 correspond to 1, 2.5, 5, 10, 15 and 25 min respectively after mixing. Spectrum 8 is for ZnTAP (after exposure for 1 day).

state or of the M—X bonds formed by the acido-ligand X, which leave the metal ion after the potential barrier of reaction (7) is overcome, is much less. Thus the rate constants may vary under comparable conditions by a factor of thousands upon the nature of the metal and with no correlation with the complex stability constant, by a factor of hundreds on the nature of the solvent and the porphyrin ligand and by a factor of ten on the nature of the leaving acido ligand [4].

3.1.2. Interaction with meso-nitrogen atoms

Unlike common porphyrins, azaporphyrins have additional donor centres, namely *meso*-nitrogen atoms. Their donor properties are very weak but more pronounced than those of the internal nitrogen atoms. It was shown that one of four *meso*-nitrogen atoms interacts with acids forming first an H associate $H_2TAPH^+ \cdots A$ with $pK_a = -0.15$ in AcOH [80]. The interaction with Lewis acids produces the same changes in the UV–visible spectra of H_2TAP [80] and H_2Pc [81,82] as the interaction with common acids, i.e. *Q* band shifts to the red. These changes are not the result of an interaction with the Lewis acids themselves but with the common acids formed by hydrolysis in the presence of traces of water [83]. A weak interaction of the *meso*-nitrogen atoms with the metal is also possible but, as was shown recently for tetratin-*star*-Ni-(porphyrazin)S_8 (tetrakis-(S,S,N-dibutyltin)-octathiolatotetraazaporphyrinatonickel(II) $NiTAP(S(SnBu_2)S)_4$) [84], this interaction does not produce changes in the position of the *Q* band, but shifts the *B* band hypsochromically. The coordination bond in such complexes is very weak and complexes can be

isolated only when the metal atom is attached to the porphyrin molecule by an additional strong coordination bond as for example with S atoms in the β positions of pyrrole rings of $NiTAP(S(SnBu_2)S)_4$.

As we shall show later, such weak complexes may be formed as intermediates in the incorporation of metals into azaporphyrins.

3.2. Complexation in non-aqueous media

3.2.1. The influence of aza substitution

For the first time, the effect of aza substitution on complexation (4) has been investigated with tetraazaporphyrins (H_2TAP and its octaphenyl derivative H_2TAPPh_8) in pyridine [85–88]. Subsequently this reaction was also studied for tetrabenzoporphine (H_2TBP) [89], its monoaza- and triaza-derivatives (H_2MATBP and H_2TATBP) [90] and for tetrabutyl-substituted phthalocyanine ($H_2Pc^tBu_4$) [91], and also for the series of alkyl-substituted azaporphyrins: 3,7,13,17-tetramethyl-2,8,12,18-tetrabutylporphine ($H_2P(MeBu)_4$), 3,7,12,18-tetramethyl-2,8,13,17-tetrabutyl-5-monoazaporphine ($H_2MAP(MeBu)_4$), 3,7,13,17-tetramethyl-2,8,12,18-tetrabutyl-5,15-diazaporphine ($H_2DAP(MeBu)_4$), 5,15-diazaoctamethylporphine-(H_2DAPMe_8), tetra(*tert*-butyl)tetraazaporphine ($H_2TAP^tBu_4$) and tetra(tetramethylene)tetraazaporphine ($H_2TAP(C_4H_8)_4$) [90,92]. Kinetic parameters for the reaction of these ligands with Cu and Zn acetates in pyridine are represented in Table 4.

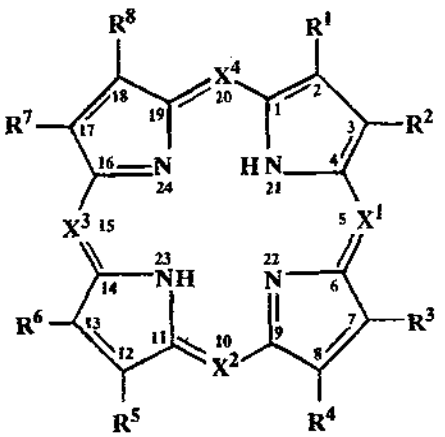

Ligand	R^1	R^2	R^3	R^4	R^5	R^6	R^7	R^8	X^1	X^2	X^3	X^4
$H_2P(MeBu)_4$	Bu^n	Me	Me	Bu^n	Bu^n	Me	Me	Bu^n	CH	CH	CH	CH
$H_2MAP(MeBu)_4$	Bu^n	Me	Me	Bu^n	Me	Bu^n	Bu^n	Me	N	CH	CH	CH
$H_2DAP(MeBu)_4$	Bu^n	Me	Me	Bu^n	Bu^n	Me	Me	Bu^n	N	CH	N	CH
H_2DAPMe_8	Me	Me	Me	Me	Me	Me	Me	Me	N	N	N	N
$H_2TAPBu^t_4$	H, Bu^t		H, Bu^t		H, Bu^t		H, Bu^t		N	N	N	N
$H_2TAP(C_4H_8)_4$	$-(CH_2)_4-$		$-(CH_2)_4-$		$-(CH_2)_4-$		$-(CH_2)_4-$		N	N	N	N
H_2TAPPh_8	Ph	Ph	Ph	Ph	Ph	Ph	Ph	Ph	N	N	N	N

In the series of benzoporphyrins, substitution of one methine group (−CH=) with a nitrogen atom increases the complexation rate with Zn and Cu acetates by about a factor of 20. The further substitution of the second and the third methine groups by nitrogen atoms exerts a lesser influence on the complexation rate, increasing it only by three times for the Zn complex and by 18 times for the Cu complex. The introduction of the fourth nitrogen atom, i.e. transition to phthalocyanine again accelerates the reaction considerably [91]. The overall increase in the complexation rate due to the introduction of four *meso*-nitrogen atoms is about 5000 times. The same effect is observed in the series of alkyl-substituted porphyrins and this was explained by an increase in the degree of polarisation of the N−H bonds as a result of the electron withdrawing influence of the *meso*-nitrogen atoms [85,86,90,92]. Consideration of the aza substitution effect in the series of alkylated porphyrins reveals that this is not the only factor which can accelerate complexation. The introduction of the first nitrogen atom (the transition from $H_2P(MeBu)_4$) to $H_2MAP(MeBu)_4$) increases complex formation rate in the case of $Cu(OAc)_2$ in pyridine by 320 times, whereas the introduction of two nitrogen atoms (transition to $H_2DAP(MeBu)_4$) increases it by only ten times. This indicates that account must be taken of the large steric distortions of the planar skeleton which are observed in the monoaza-substituted porphyrins; the deviations from planarity reach 0.03 nm [14,19] and are especially significant for the coordinating nitrogen atoms. For monoaza-substituted derivatives, the acceleration of metal incorporation is determined first of all by the steric factor which is especially pronounced for alkyl-substituted derivatives with a more flexible skeleton. One can suppose that the more

Table 4
Influence of aza substitution on the kinetic parameters for the complexation of alkyl and benzo-substituted porphyrins with Cu and Zn acetates in pyridine ($[H_2AP]^0 = 1 \times 10^{-5}$ M; $[M(OAc)_2]^0 = 3 \times 10^{-4}$ M)

Complex	n	$k_{eff}^{298\ K} \times 10^4$ (s^{-1})	E_a (kJ mol^{-1})	$\Delta S \neq$ (J $mol\ K^{-1}$)	Reference
ZnTBP	1	0.028	88	8	[89]
CuTBP	1	0.31	63	−59	[89]
ZnMATBP	1.3	0.526	86	−287	[90]
CuMATBP	0.5	6.12	23	−241	[90]
ZnTATBP	1	1.48	98	−279	[90]
CuTATBP	1	109	42	−149	[90]
$ZnPc^tBu_4$	1	135	52	−46	[91]
$CuPc^tBu_4$	1	2440	47	−39	[91]
$CuTAP(C_4H_8)_4$	0.68	0.38	44	−191	[90]
$CuTAP^tBu_4$	0	2.65	50	−154	[90]
$CuDAPMe_8$	0	0.0158	70	−150	[90]
$CuDAP(MeBu)_4$	0.1	0.0060	57	−174	[90]
$CuMAP(MeBu)_4$	0.1	0.180	42	−219	[90]
$CuP(MeBu)_4$	1	0.000562	74	−89	This work

Uncertainties in k_{eff} and E_a are less than 10%, and in $\Delta S \neq \pm 12$ J mol^{-1} K^{-1}.

symmetric diaza derivative is also more planar and the electronic effect becomes the determining factor. The same is true for triaza and tetraaza derivatives with more rigid skeletons. The enhancement of complex formation rates for azaporphyrins is accompanied by lowering of the activation energies E_a and activation entropies $\Delta S^{\neq}$. The latter implies a stronger solvation of the transition state.

Comparison of the rate constants in the series of aza-substituted tetrabenzoporphyrins and porphyrins shows that aza substitution has a greater impact on the coordinating properties of the porphyrin ligand than benzo substitution which was also supposed [89] to increase the coordination activity of the porphyrin ligand owing to polarization of the N—H bonds. This is in line with the fact that tetrabenzo substitution increases the acidity constant by four orders of magnitude whereas tetraaza substitution increases acidity by ten orders if magnitude [74,75].

The high reactivity of tetraazaporphyrins in coordination with metal ions in pyridine compared with porphyrins is considered to be due to the polarization of the N—H bonds by the *meso*-nitrogen atoms [86]. As this factor is interconnected with both increasing aromaticity of the macrocycle and lowering of the lowest unoccupied molecular orbital as a result of aza substitution [28,30,31], it is beneficial to stabilization of the TAP^{2-} anion formed in the transition state of the reaction. Substituents in the tetraazaporphyrin pyrrole rings also have an influence on its stability and on the reactivity of tetraazaporphyrins in complexation.

3.2.2. The influence of pyrrole ring substituents in tetraazaporphyrins

Complexation with metal acetates in pyridine has been investigated for unsubstituted H_2TAP [86], its alkyl derivatives $H_2TAP(C_4H_8)_4$ and $H_2TAP^tBu_4$ [90,92], the aryl derivative H_2TAPPh_8 [85] and the benzo derivative $H_2Pc^tBu_4$ [91]. Recently tetrahalogen-substituted derivatives were also studied [76,93].

As one can see in Table 5 alkyl substitution retards complexation. If the electron density on the coordinating nitrogen atoms was the factor determining the reactivity, then alkyl groups as electron-donating substituents should accelerate the reaction. Such an effect is observed for common porphyrins where ethioporphyrine ($H_2P(MeEt)_4$) coordinates with $Cu(OAc)_2$ in EtOH 3.5 times more rapidly than unsubstituted H_2P [79]. At the same time, alkyl substituents increase the covalency and strength of the N—H bonds and their inhibiting effect for tetraazaporphyrins (as well as for tetrabenzoporphyrins [89,94]) shows that in this case the rupture of the N—H bonds is the determining factor. For aryl substituents in H_2TAPPh_8 a similar but weaker effect as for the alkyl groups is observed [85].

The introduction of electron-withdrawing substituents, such as halogen atoms, drastically accelerates metal incorporation which proceeds in pyridine almost instantaneously with rates which are too fast to be measured by conventional kinetics methods [76,93]. Such a strong halogen influence is explained by the steeply raised ionic character of the N—H bonds. H_2TAPBr_4 has an acidity five orders of magnitude higher than that of H_2TAP (pK_1 in DMSO 7.26 and 12.35 respectively). Benzo substitution also increases the acidity of the N—H bonds (by a factor of 10^5 for porphyrins and by a factor of 10^2 for tetraazaporphyrins [74]) and also the reactivity of the ligands in complex formation. It was supposed [76] that stabilization of the

Table 5
Kinetic parameters for complexation of substituted tetraazaporphyrin ligands with metal acetates in pyridine ($[H_2AP]^0 \approx 1 \times 10^{-5}$ M; $[M(OAc)_2]^0 = 3 \times 10^{-4}$ M)

Complex	n	$k_{eff}^{298\ K}$ (10^4 s^{-1}) (s^{-1})	E_a (kJ mol^{-1})	$\Delta S \neq$ (J $mol\ K^{-1}$)	Reference
CuTAP	1.2	3470	118	+116	[86]
ZnTAP	0.90	17.38	44	−161	[86]
CdTAP	0.89	10.47	75	−57	[86]
CoTAP	0.82	4.79	60	−112	[86]
MnTAP	0.49	1.07	57	−136	[86]
NiTAP	0.99	0.050	85	−64	[86]
MgTAP	0.50	0.000096	115	−9	[88]
$CuTAPPh_8$	0.13	6.03	51	−145	[85]
$ZnTAPPh_8$	0.17	2.79	53	−141	[85]
$CdTAPPh_8$	0.15	2.00	15	−264	[85]
$NiTAPPh_8$	0.12	1.20	25	−229	[85]
$CoTAPPh_8$	0.16	1.10	56	−147	[85]
$MnTAPPh_8$	0.02	0.37	54	−158	[85]
$CuTAP(C_4H_8)_4$	0.68	0.32	44	−191	[90]
$ZnTAP(C_4H_8)_4$	1.00	0.132	57	−160	[90]
$CdTAP(C_4H_8)_4$	0.88	0.099	55	−167	[90]
$CoTAP(C_4H_8)_4$	1.05	0.00765	79	−100	[92]
$CuTAP^tBu_4$	0	2.65	50	−154	[90]
$CuPc^tBu_4$	1	2490	47	−38	[91]
$ZnPc^tBu_4$	1	135	52	−46	[91]
$CdPc^tBu_4$	1	120	57	−31	[91]
$CoPc^tBu_4$	1	19.2	72	5	[91]
$NiPc^tBu_4$	1	3.3	62	−52	[91]

Uncertainties in k_{eff} and E_a are less than 10%, and in $\Delta S \neq \pm 12$ J mol^{-1} K^{-1}.

dianion TAP^{2-} in the transition state, by electron-withdrawing substituents or by annelated benzene rings, facilitates cleavage of the N—H bonds and speeds up metal incorporation.

Fig. 6 displays the correlation between the acidity constants in DMSO (pK_1) of H_2P, H_2TBP, H_2Pc and azaporphyrins and the rate constants ($\log k_v$) in the reaction of these ligands with Zn and Cu acetates in pyridine. The existence of such correlation substantiates that the acidity of the N—H bonds is the main factor determining the reactivity of tetraazaporphyrins in pyridine.

Another factor having a large impact on the ease of proton removal from the reaction centre is the nature of the solvent.

3.2.3. The influence of solvent

The reaction of H_2TAP with metal acetates was investigated in pyridine [86], EtOH [87], DMF [95], AcOH [95] and MeCN [96]. The solvent effect on the reactivity of $H_2Pc^tBu_4$ in complex formation was studed in pyridine [91], AcOH and pentanol [97].

From Table 6, one can see that the highest reactivity for tetraazaporphyrin ligands

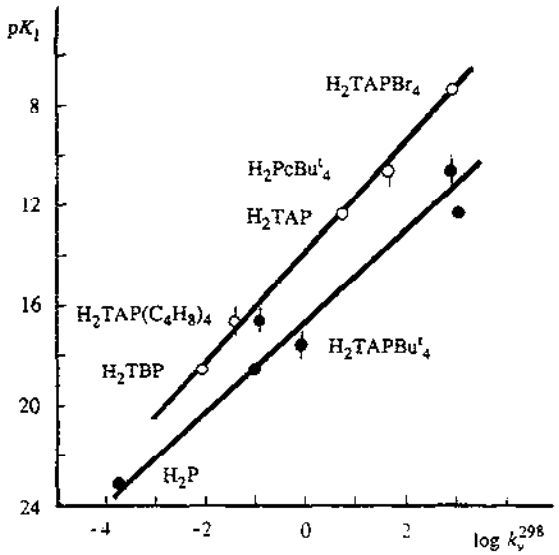

Fig. 6. Correlation between acidity ($pK_1^{298\,K}$ in DMSO) of porphyrin and tetraazaporphyrin ligands and their reactivity in complexation with Zn (○) and Cu (●) acetates in pyridine ($k_v^{298\,K}$). ([$M(OAc)_2$]^0 = 3×10^{-4} M).

is observed in the strongly coordinating pyridine which forms the most strong bonds with the metal salt (M—solv) and where the common porphyrins show the least reactivity. Conversely in the weakly coordinating acetic acid (the most favourable solvent for porphyrin complexation), for H_2TAP and $H_2Pc^tBu_4$ the complexation rates are the lowest. For H_2TAP the rate constant for complexation with Cu acetate in pyridine is 8300 times higher than in EtOH, whereas for $H_2P(MeEt)_4$ the rate constant in EtOH is 10 000 times higher than for the structurally similar $H_2P(MeBu)_4$ in pyridine. This confirms strongly the suggestion that in azaporphyrins the cleavage of the N—H bonds determines the kinetic parameters for complexation and not the rupture of M—solv bonds as takes place in common porphyrins. In pyridine the complexation rate constants for H_2TAP and $H_2Pc^tBu_4$ are hundreds and even thousands of times higher than for common porphyrin ligands. In solvents with weakly basic properties (DMF, EtOH and MeCN) and especially in the proton-donating solvent (AcOH) the reactivity of tetraazaporphyrin ligands is comparable with the reactivity of common porphyrins or is even less.

In order to appreciate better the reasons for such solvent effects the difference between the structures of the coordination centre N_4H_2 in porphyrins and tetraaza-porphyrins must be taken into account (see Section 2.2.2). The LS structure with covalent localized N—H bonds exists in common porphyrin ligands whereas in tetraazaporphyrins, because of better conditions for strong intramolecular H bonding the delocalized structures of the reaction centre (HS or US) are also possible. The solvation of the reaction centre in tetraazaporphyrins determines its structure. The

Table 6
Kinetic parameters of the formation of Cu and Zn complexes of porphyrin and tetrazaporphyrin ligands in different solvents ($[H_2AP]^0 \approx 1 \times 10^{-5}$ M; $[MX_2]^0 = 3 \times 10^{-4}$ M)

Complex	Solvent	MX_2	$k_{eff}^{298\ K} \times 10^4$ (s^{-1})	E (kJ mol^{-2})	$\Delta S \neq$ (J $mol\ K^{-1}$)	Reference
CuTAP	Pyridine	$Cu(OAc)_2$	3470	118	+116	[86]
		$CuCl_2$	5.37	20	−250	[95]
	AcOH	$Cu(OAc)_2$	2.02	30	−250	[95]
	EtOH	$Cu(OAc)_2$	1.04	57	−141	[87]
	DMF	$CuCl_2$	0.45	52	−160	[95]
ZnTAP	Pyridine	$Zn(OAc)_2$	17.38	44	−161	[86]
	EtOH	$Zn(OAc)_2$	6.1	45	−163	[87]
	AcOH	$Zn(OAc)_2$	0.026	50	−190	[93]
	+1% pyridine		0.081	52	−180	[93]
	+60% pyridine		2.87	62	−106	[93]
	MeCN		0.0211	13	−206	[96]
$CuPc^tBu_4$	Pyridine	$Cu(OAc)_2$	2416	47	−38	[91]
	AcOH		7.83	32	−136	[97]
	Pentanol		0.19	90	+16	[97]
ZnP	EtOH	$Zn(OAc)_2$	0.92			[4]
CuP	EtOH	$Cu(OAc)_2$	1.65	55	−67	[79]
$CuP(MeEt)_4$	EtOH	$Cu(OAc)_2$	5.82	56	−50	[79]
$CuP(MeBu)_4$	Pyridine	$Cu(OAc)_2$	0.000562	74	−89	This work
ZnTBP	Pyridine	$Zn(OAc)_2$	0.028	88	+8	[89]
	MeCN	$Zn(OAc)_2$	0.037	33	−142	[96]
CuChl	AcOH	$Cu(OAc)_2$	15.9	44	−79	[79]
	EtOH		4.95	44	−96	[79]
	Pentanol		1.67	113	+126	[79]
	DMF		0.108	79	−8	[79]
	Pyridine		0.0276	96	+37	[79]

Uncertainties in k_{eff} and E_a are less than 10%, and in $\Delta S \neq \pm 10$ J $mol\ K^{-1}$.

solvents which are able to form H bonds (alcohols) and especially proton-donating solvents (acids) solvate the reaction centre through formation of H bonds with the internal nitrogen atoms (aza type) and is reduces the internal H bonding, increases the covalency of the N—H bonds and the reaction centre attains the LS structure (Figs. 7(a) and 7(b)). Such solvation hinders the removal of protons from the reaction centre and, in spite of the greater lability of the M—solv bonds in these solvents, the reaction proceeds slowly. If one takes into account that aza substitution decreases the overall elecron density on the internal nitrogen atoms [28,29], then it will be clear why the LS structure of tetraazaporphyrins appears to be less active than such a structure for porphyrins. The complexation rate constant with Cu acetate in EtOH is four times lower for H_2TAP than for H_2P. The reactivity of H_2TAP in comparison with chlorophyllic acid a (H_2Chl) is less in EtOH (12 times) and in AcOH (eight times), is slightly higher in DMF (four times) and is higher in pyridine by five orders of magnitude. The same is observed for the phthalocyanine ligand $H_2Pc^tBu_4$. The

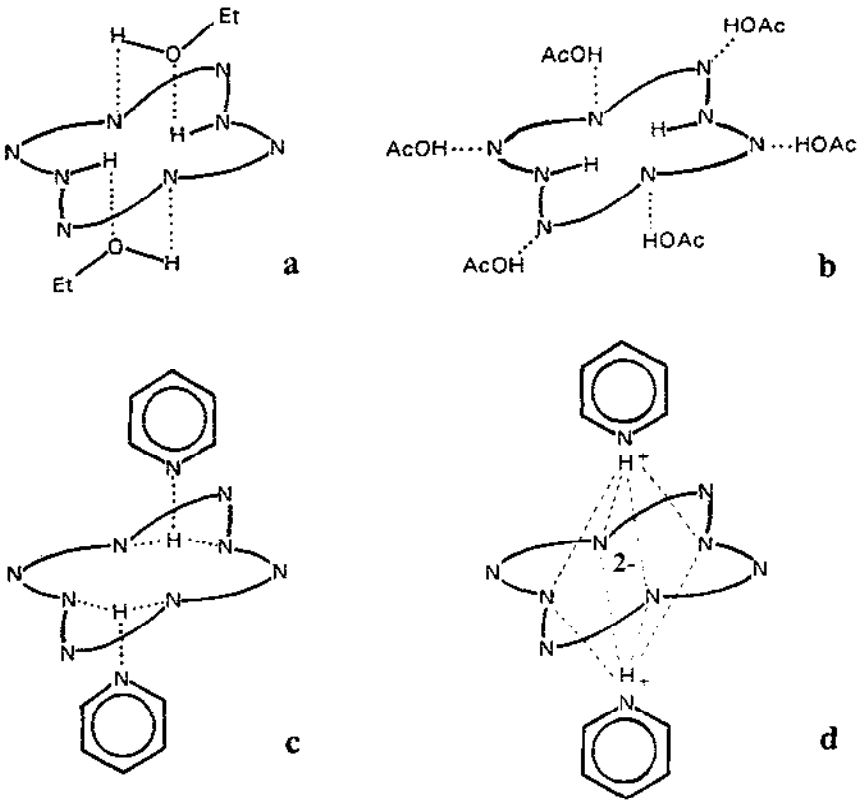

Fig. 7. Solvation of the H_2TAP reaction centre in (a) EtOH, (b) AcOH, (c) pyridine and (d) the structure of the pyridinium salt.

basic solvents such as pyridine enhance the ionization of the N—H bonds and the reaction centre attains the more reactive US structure (Fig. 7(c)).

This solvation effect on the reaction centre structure in H_2TAP is also reflected in the UV–visible spectra (Table 2). The nature of the solvent only slightly affects the energy of the *Q* bands and their splitting, but greatly influences the *B* band which is shifted in pyridine about 500–600 cm^{-1} bathochromically compared with solutions in EtOH and AcOH. This reflects increasing electron density on the internal nitrogen atoms in the US structure compared with the LS and the destabilization of the a_{2u} orbital which have non-zero coefficients on these atoms and is responsible for the *B* transition. The observed splitting of the *B* band in pyridine (565 cm^{-1}) is about half that in EtOH or AcOH (1230–1390 cm^{-1}) and this correlates well with the *B*-band splitting predicted by Mamaev et al. [53] for US (632 cm^{-1}) and LS (1613 cm^{-1}) models of the reaction centre in H_2Pc.

The observed low activation entropy values confirm the important role of the solvent in complex formation and are suggestive of more pronounced solvation of the transition state in tetraazaporphyrins. The stronger solvation of the reaction

centre and of the metal ion can both contribute to lowering the $\Delta S^{\neq}$ values. For common porphyrins the main energy expenses are connected with the cleavage of the M—solv bonds [98]. This is why E_a and $\Delta S^{\neq}$ values are lower in weakly coordinating solvents (the transition state is closer to the initial products) and higher in strongly coordinating solvents such as pyridine where the transition state is closer to the end products of the reaction and the solvate sphere of the metal ion is already destroyed [79]. For tetraazaporphyrins the values of E_a and $\Delta S^{\neq}$ are similar, in both types of solvent which differ greatly in their ability to coordinate with the metal ion, and strongly solvate the tetraazaporphin ligand reaction centre owing to their distinct basic (pyridine) or proton–donor properties (EtOH and AcOH). This indicates that in tetraazaporphyrins the desolvation of the reaction centre and the cleavage of the N—H bonds provide the principal contribution to the activation parameters and that the stability of the solvate sphere of the metal ion is less important at the activation stage. At the same time the delocalized structure existing in basic solvents is more reactive in complex formation than is the localized structure in proton-donor solvents. In the case of ZnTAP replacing AcOH with pyridine speeds up complexation by almost 700 times but only slightly decreases the activation energy by 6 kJ mol^{-1} and $\Delta S^{\neq}$ increases by 29 J mol^{-1} K^{-1}. In MeCN because of its poor ability to solvate the donor centre and its low basicity, the reaction centre of H_2TAP is not shielded by solvation and the activation energy is about a quarter of that in pyridine or AcOH [96]. However, it does not accelerate complexation and the rate constant is almost the same as in AcOH, the result which can be expected for the same LS structure.

Recently very interesting data were obtained for the reaction of Zn acetate with H_2TAP and its tetrahalogen derivatives (H_2TAPBr_4, H_2TAPCl_4 and H_2TAPF_4) in pyridine–AcOH mixtures [93]. The almost instantaneous reaction of the halogenated H_2TAP in pure pyridine is retarded strongly in the presence of AcOH (Table 7). In the mixture containing 60% AcOH, the complexation rate is retarded by 30 times for H_2TAP and by more than 5000 times for H_2TAPBr_4. In a mixture of such composition the reactivity of the ligands increases with increasing electronegativity of the substituents:

$$H_2TAP < H_2TAPBr_4 < H_2TAPCl_4 < H_2TAPF_4$$

This order corresponds to that expected for the delocalized HS or US reaction centre structures. As the increasing ionic character in the N—H bonds is the determining factor, it speeds up the reaction. In a mixture containing only 1% pyridine, the complexation rate decreases further and is especially pronounced for the halogen derivatives (by 35 times for H_2TAP and by 360 times for H_2TAPF_4). As a result the order of reactivity becomes the opposite:

$$H_2TAPF_4 < H_2TAPCl_4 < H_2TAPBr_4 < H_2TAP$$

Such an order corresponds to that expected for the LS structure. Increasing the electron density on the aza nitrogen atoms accelerates the reaction.

The solvation of the reaction centre determining its structure can influence not

Table 7
Kinetic parameters of the formation of Zn complexes of H_2TAP and its halogen-substituted derivatives in pyridine–AcOH mixtures [93]

Complex	Solvent	$k_v^{298\ K}$ ($s^{-1}\ M^{-1}$)	E_a (kJ mol^{-1})	$\Delta S \neq$ (J $mol\ K^{-1}$)
ZnTAP	100% AcOH	0.0087	50	−190
$ZnTAPBr_4$		0.0070	55	−185
ZnTAP	99% AcOH	0.0054	52	−180
$ZnTAPBr_4$		0.0020	78	−110
$ZnTAPCl_4$		0.0011	77	−128
$ZnTAPF_4$		0.00074	72	−146
ZnTAP	60% AcOH	0.191	62	−106
$ZnTAPBr_4$		0.197	71	−120
$ZnTAPCl_4$		0.225	54	−161
$ZnTAPF_4$		0.270	58	−147
$ZnTAPBr_4$	0.45% AcOH	931	23	−216
ZnTAP	100% pyridine	5.79	44	−161
$ZnTAPBr_4$		Very quick		
$ZnTAPCl_4$		Very quick		
$ZnTAPF_4$		Very quick		

Uncertainties in k_v and E_a are less than 10%, and in $\Delta S \neq \pm 16$ J $mol\ K^{-1}$.

only the reactivity of the tetraazaporphryin ligands in complex formation but also the reaction mechanism.

3.2.4. Pecularities of the complexation mechanism

The complex formation reactions of tetraazaporphyrins are always first order in the ligand. The order in metal salt is also often first order but in some cases it is fractional. It was proposed [85–87] that the mechanism of complexation can deviate from the typical $S_{NE}2$ mechanism (7) established for porphyrins [79] owing to the pecularities of the tetraazaporphyrin structure and two mechanisms were suggested: bimolecular and monomolecular.

3.2.4.1. Bimolecular mechanism. The complexation reaction of tetraazaporphyrine, its halogen-substituted derivatives as well as phthalocyanine has an order in metal salt approaching unity (Fig. 8) and obeys the bimolecular rate law

$$\frac{-d[H_2AP]}{dt} = k_v[H_2AP][MX_2] \tag{8}$$

The complexation proceeds according to this equation both in an acid medium (AcOH) and in a basic medium (pyridine).

In the first case, the bimolecular mechanism is the same as for common porphyrins (7); at the activation stage the metal ion loses two solvent molecules from its solvate

sphere and interacts with two aza nitrogen atoms of the reaction centre having the LS structure. Desolvation of the reaction centre also proceeds during activation but the N—H bonds themselves are only slightly elongated.

In the second case, at the activation stage, the pyridine molecules solvating the internal protons withdraw them from the macrocycle plane, increasing the negative charge on the reaction centre which has a delocalised structure. The metal ion only assists this process and the formation of the stable macrocyclic complex more than compensates the barrier for the cleavage of the M—solv bonds:

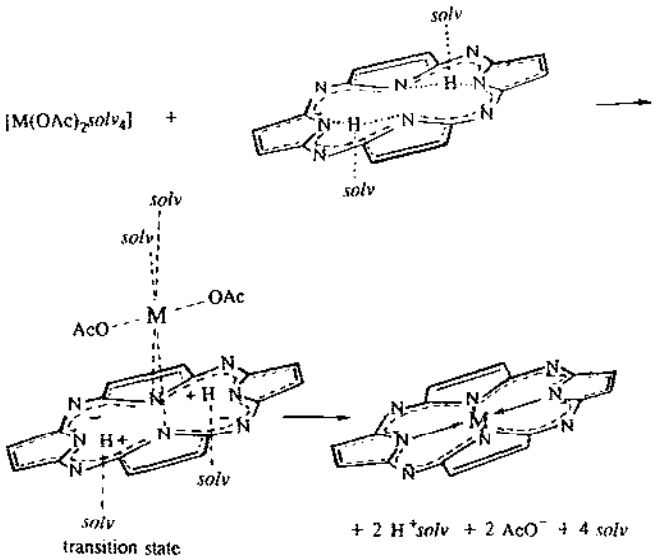

(9)

The dianion AP^{2-} does not appear as an intermediate in pyridine. Under certain conditions, interaction of the tetraazaporphyrin ligands with pyridine or other nitrogen bases can result in removal of protons from the reaction centre even without assistance of the metal ion, with formation of a pyridinium salt:

$$H_2AP + 2py \rightarrow (pyH^+)_2 \cdots AP^{2-} \quad (10)$$

where py is pyridine. Such a reaction was observed for the first time with H_2TAP, with its alkyl derivatives, and with H_2Pc by Whalley [99] who also showed that formation of such a salt can proceed as a photoinduced process. Without photoexcitation, we have not observed formation of a pyridinium salt during long-term refluxing of H_2TAP in pyridine. H_2TAPPh_8 forms such a salt more easily on standing in a pyridine solution at room temperature or on refluxing for several hours [85]. In the case of H_2TAPBr_4 with more prominent acidic properties the formation of a pyridinium salt in pure pyridine is finished in 40–60 min at room temperature and the ligand bands in the UV–visible spectrum at 570 and 637 nm disappear and a new band at 605 nm appears [76]. Changes in the UV–visible spectra accompanying the formation of pyridinium salts (Fig. 9) are similar to those for metal incorporation. This corresponds to the removal of protons from the reaction centre with a rise of

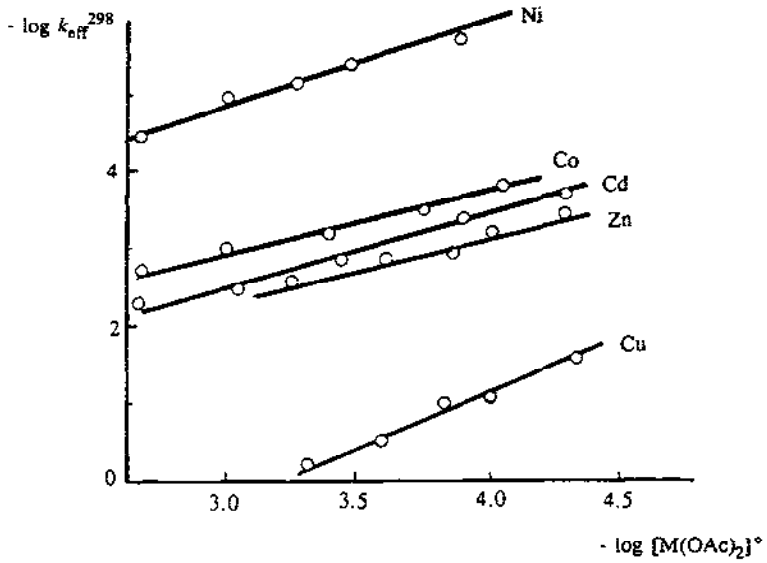

Fig. 8. Dependence of log $k_{eff}^{298\ K}$ from log[M(OAc)$_2$]^0 for the complexation of H_2TAP with metal acetates in pyridine.

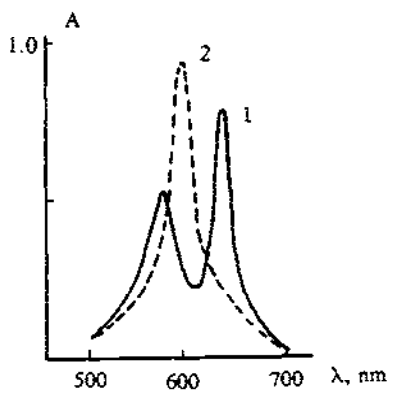

Fig. 9. UV–visible spectrum of H_2TAPBr_4 in chloroform and of its pyridinium salt $(PyH^+)_2\cdots TAPBr_4^{2-}$ in pyridine.

the ligand symmetry from D_{2h} to D_{4h} (Fig. 7(d)). Vul'fson et al. [100] observed the formation of H_2Pc salts with different amines and found that they can be formed only in non-protonating polar solvents. Pyridinium salts are not active in complexation with metal salts [85,93]. This indicates that even the pyridinium salt is not a true ionic compound. As has been shown [75], the dianion TAP^{2-} only forms in good ionizing media such as DMSO in the presence of the strong base $(N^nBu_4)^+OH^-$, when the internal protons are removed as a molecule of H_2O and two cations $(N^nBu_4)^+$ stabilize the dianion TAP^{2-}.

If such a dianion was formed, then owing to its high complexation reactivity one should expect a monomolecular reaction and a dissociative mechanism. Monomolecular processes are in fact observed, in some cases, for tetraazaporphyrin ligands, but under conditions where the formation of a dianion does not occur.

3.2.4.2. Monomolecular mechanism. In some cases complex formation (1) deviates from the bimolecular law (8). The order (n) of the reaction in metal salt, determined according to equation (6) as the slope of the log k_{eff} dependence with log[MX_2] can be fractional and considerably less than unity (Tables 4 and 5). The complexation of H_2TAP with Zn acetate was first order in metal salt in AcOH [76] and MeCN [96] but fractional in pyridine ($n=0.90$) [86] and in EtOH ($n=0.40$)[87]. The rate of reaction of H_2TAPPh_8 with metal acetates in pyridine depends only slightly on the metal salt concentration ($n=0.02$–0.17 (Fig. 10)) [87] and for monoaza- and diaza-substituted porphyrins the order in metal salt is zero (Fig. 11) [90]. It was proposed [85] that in azaporphyrins not only do the internal nitrogen atoms take part in coordination but also the *meso*-nitrogen atoms which form a weak intermediate complex of the amine type with metal salt (see also Section 3.1.2.) with an equilibrium constant K in accordance with the equation

$$H_2TAP + [M(OAc)_2solv_4] \rightleftharpoons [H_2TAPM(OAc)_2solv_3] + solv \qquad (11)$$

This intermediate complex can convert to MTAP according to a monomolecular mechanism with rate constant k_1:

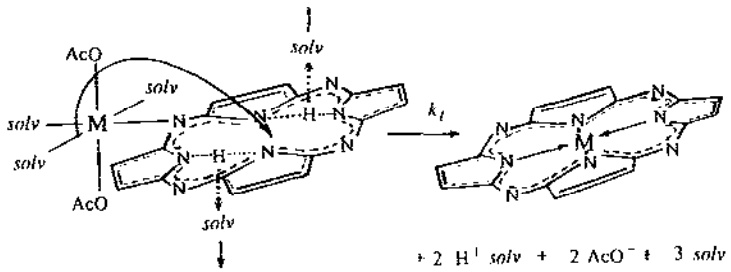

(12)

The monomolecular mechanism (12) competes with the usual bimolecular mechanism (rate constants k_2 and k_3) [87,88]:

$$H_2TAP + [M(OAc)_2solv_4] \xrightarrow{k_2} MTAP + 2AcOH + 4solv \qquad (13)$$

$$[H_2TAPM(OAc)_2solv_3] + [M(OAc)_2solv_4] \xrightarrow{k_3} [MTAPM(OAc)_2solv_3] + 2AcOH + 4\ solv \qquad (14)$$

Since coordination with the *meso*-nitrogen atoms in the intermediate is weak, it was assumed that $k_2=k_3$ and the following equation for the observed constant k_{eff}

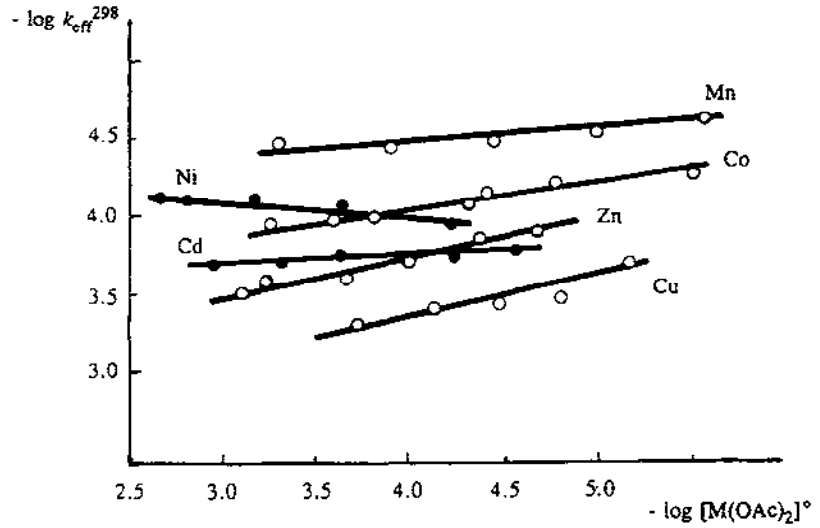

Fig. 10. Dependence of log $k_{eff}^{298\ K}$ from log[M(OAc)$_2$]° for the complexation of H_2TAPPh_8 with metal acetates in pyridine.

was deduced [87]:

$$k_{eff}=\frac{K[MX_2]^\circ(k_1+k_2[MX_2]^\circ)+k_2[MX_2]^\circ}{K[MX_2]^\circ+1} \tag{15}$$

Using this equation the values of K, k_1 and k_2 were determined from experimental kinetic data [34]. For the reaction between H_2TAP and Zn acetate in EtOH and pyridine, K is equal to 7020 M^{-1} and 1460 M^{-1} respectively, k_1 to 8.71×10^{-4} s^{-1} and 25.4×10^{-4} s^{-1} respectively, and k_2 to 0.11 s^{-1} M^{-1} and 4.14 s^{-1} M^{-1} respectively. Since pyridine assists the cleavage of N—H bonds, the rate constants for both mechanisms are higher in pyridine than in EtOH. In as much as the M—py bond is stronger than M—EtOH, the formation constant K of intermediate is less in pyridine. The replacement of EtOH by pyridine accelerates the monomolecular reaction by only three times whereas the bimolecular reaction increases 40 times. This reflects the considerable changes in the solvate sphere of the metal ion in the intermediate of the monomolecular reaction (12) whereas in the transition state of the bimolecular reaction (7) these changes are smaller. Strong solvation of the reaction centre by EtOH especially binders the bimolecular reaction. Thus in 300-fold excess of Zn acetate the bimolecular mechanism accounts for 86% of the overall output in pyridine and only 29% in EtOH.

The structure of the ligand also influences the complexation mechanism. Aryl substituents strengthen the shielding of the reaction centre by solvation and alkyl substituents increase the electron density on the *meso*-nitrogen atoms. These factors favour the monomolecular mechanism. The same is also true for monoazaporphyrins and diazaporphyrins where *meso*-nitrogen atoms are more basic than in tetraazaporphyrins.

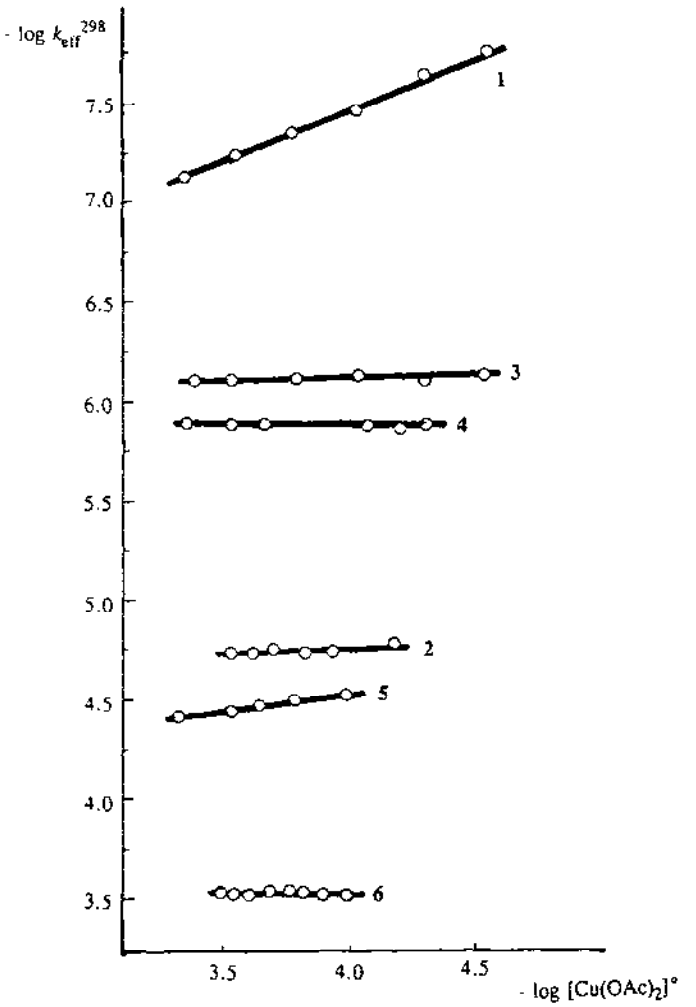

Fig. 11. Dependence of log $k_{eff}^{298\ K}$ from log[Cu(OAc)$_2$]° for the complexation of alkylsubstituted azaporphyrins with Cu acetate in pyridine: line 1, $H_2P(MeBu)_4$; line 2, $H_2MAP(MeBu)_4$; line 3, $H_2DAP(MeBu)_4$; line 4, H_2DAPMe_8; line 5, $H_2TAP(C_4H_8)_4$; line 6, $H_2TAP^tBu_4$.

In other factor which influences the kinetic parameters and the complexation mechanism is the nature of metal ion and of the anion.

3.2.5. The influence of the nature of the metal ion

The metal ion influence on complexation was studied for H_2TAP [86], H_2TAPPh_8 [85], $H_2TAP(C_4H_8)_4$ [90], $H_2Pc^tBu_4$ [91] in pyridine and also for H_2TAP in EtOH [87]. Usually reactions with acetates were investigated (M = Co(II), Ni(II), Cu(II), Zn(II), Cd(II), Mn(II) or Mg(II)).

Metal ions can be arranged in the following series in accordance with their activity

to complexing with H_2TAP in pyridine:

$$Cu(II) > Zn(II) > Cd(II) > Co(II) > Mn(II) > Ni(II) \gg Mg(II)$$

A comparison of this sequence with the stability of MTAP in acid media [101],

$$Co(II) \gg Ni(II) > Cu(II) > Zn(II) \gg Mg(II) > Cd(II)$$

reveals that the rates of metal incorporation do not depend on the degree and nature of the interaction between the metal ion and the macrocyclic ligand. They are determined mainly by the pecularities of the transformation of the coordination sphere of the metal salt in the transition state and by steric factors [86]. This is confirmed by the existence of a kinetic compensation effect in a series of tetraazaporphyrins (Fig. 12).

The dependence of the complexation rates for the tetraazaporphyrin ligands on the nature of the metal ion is similar to that observed for common porphyrins [1–4]. However, the difference in formation rates between Zn, Cd and Co complexes is unusually small because the stability of the M—solv bonds has a lesser impact on

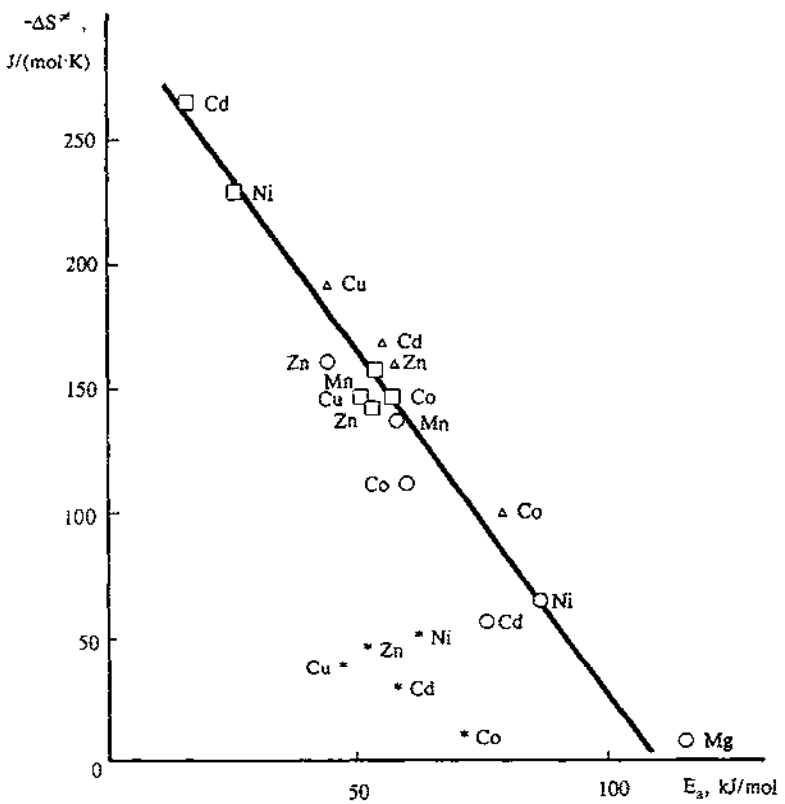

Fig. 12. Kinetic compensation effect in the complexation of tetraazaporphyrin ligands with metal acetates in pyridine: ○, H_2TAP; △, $H_2TAP(C_4H_8)_4$; □, H_2TAPPh_8; *, $H_2Pc^tBu_4$.

the complex formation of MTAP [86]. The rate sequence observed for H_2TAPPh_8, $H_2TAP(C_4H_8)_4$ and $H_2Pc^tBu_4$ in pyridine are the same as for H_2TAP. The lesser influence of the metal observed for H_2TAPPh_8 was explained in accordance with the monomolecular mechanism (12), where the solvate sphere of the metal ion in the intermediate is already strongly transformed and therefore has less impact on the limiting stage of the reaction [85].

It is remarkable that the reactivity of Cu acetate in complexation with H_2TAP and $H_2Pc^tBu_4$ in pyridine is 200–300 times higher than that of Zn acetate. For porphyrins this difference does not exceed ten times [4]. The unusually high reactivity of Cu acetate in complexation with H_2TAP was explained by tetragonal distortion of the solvate sphere in the transition state [86]. On approaching the planar macrocyclic ligand, the Cu^{2+} ion which feels the negative charge field of the macrocycle reaction centre having a US structure, strives for tetragonal coordination and loses four pyridine molecules, forming the reactive planar configuration with two bidentate acetate ligands $[H_2TAPMeCO_2CuO_2CMe]^{\neq}$ and then falls into the reaction cavity of the macrocycle with the loss of two molecules of AcOH. The large positive $\Delta S^{\neq}$ value and high E_a value correspond to strong desolvation of the transition state. In the case of Cu chloride, the tetragonal distortion of *cis*-$[CuCl_2py_4]$ results in formation of the less active *trans*-$[Cupy_4Cl_2]$ with D_{4h} symmetry and four pyridine molecules in one plane [102]. As a result, the reaction proceeds 650 times more slowly than with copper acetate and deviating from the bimolecular mechanism. The same effect is observed for $H_2Pc^tBu_4$ in pyridine: the replacement of Cu acetate by chloride retards the complexation rate by 350 times [91]. The addition of NH_4ClO_4 to Cu acetate solution causes transformation of $[Cu(OAc)_2py_4]$ to $[Cupy_4](ClO_4)_2$ having a smaller reactivity [97] and the complexation rate is also retarded 3000 times and $\Delta S^{\neq}$ decreases from -38 to -107 J mol^{-1} K^{-1}, reflecting the smaller desolvation of the transition state.

Cu acetate, which shows greater reactivity than Zn acetate in pyridine, appears to be less active in EtOH and AcOH. The reason for such a "loss" of reactivity is the dimerization of Cu acetate in these solvents. Whereas all transition metal acetates investigated exist in a monomeric form in EtOH and AcOH – $[M(OAc)_2solv_4]$ [98], Cu acetate is predominantly in the dimeric form $[Cu_2(OAc)_4]$ [103,104]. This dimeric form was shown to be unreactive in complexation with porphyrins [105] and is also responsible for underestimation of the true rate constants for reaction with tetraazaporphyrins [87,96] and phthalocyanines [97]. Calculations of bimolecular rate constants with regard to the monomer and not overall concentration have shown that $[Cu(OAc)_2solv_4]$ is more active than $[Zn(OAc)_2solv_4]$ also in EtOH and AcOH [76,87,95].

In some cases, the originally formed complex MTAP immediately undergoes a further transformation, e.g. in the case of Mn acetate complexation. In pyridine the initially formed $py_2Mn^{II}TAP$ is oxidized to the μ-oxo-dimer $O(pyMn^{III}TAP)_2$ while in EtOH the monomeric Mn(III) complex is formed, $(AcO)Mn^{III}TAP$ [86,87].

The high coordinative reactivity of H_2TAP allows one to investigate the rare reaction of Mg incorporation [88]. Usually complexes of porphyrins and Mg(II) are only obtained in template synthesis. The kinetics of Mg(II) incorporation in

porphyrins has been studied only for the dimethyl ester of deuteroporphyrin [106]. The reaction of MgTAP formation was studied in pyridine where the inner coordination sphere of the Mg(II) ion is unlike transition metal ions formed by six pyridine molecules and anions (acetate and perchlorate) are in the outer coordination sphere: $[Mg(py)_6](OAc)_2$ and $[Mg(py)_6](ClO_4)_2$ [88]. Thus the coordination of H_2TAP with Mg(II) proceeds by a factor of 10^5 more slowly than with Zn(II) or Cd(II). At the same time H_2TAP is a factor of 10^4 more active in complexing with Mg than are common porphyrins. The tetrabromo-substituted derivative H_2TAPBr_4 is even more active and was suggested as an analytical reagent for the quantitative determination of Mg^{2+} and some other ions in pyridine solutions [107].

3.3. Complexation of tetraazaporphyrins in aqueous media

Whereas kinetic studies of metal incorporation with common porphyrin ligands were often carried out with water-soluble compounds in aqueous media [2,3], the coordination properties of tetraazaporphyrin ligands were until recently investigated only in non-aqueous media. The only exception was the brief report of Schiller and Bernauer [108] on the reaction of tetrasulphophthalocyanine ($H_2Pc(SO_3H)_4$) with Cu^{2+} and Zn^{2+} ions in water. In the last few years, water-soluble sulpho derivatives of tetraazaporphyrins have become available; tetrasulfotetraazaporphine ($H_2TAP(SO_3H)_4$) [109] and octasulphophenyltetraazaporphine ($H_2TAP(C_6H_4SO_3H)_8$) [110]. Complexation with metal acetates in water and aqueous media was studied by Timofeeva et al. [111] for $H_2TAP(SO_3H)_4$ and by Petrov and coworkers [112–114] for $H_2TAP(C_6H_4SO_3H)_8$.

3.3.1. The state of tetraazaporphyrin ligands in water

Sulpho derivatives of tetraazaporphyrins and phthalocyanines are soluble in water. However, $H_2TAP(SO_3H)_4$ and $H_2Pc(SO_3H)_4$ aggregate in water solution presumably forming dimers [111,115]. They are very stable (for $(H_2Pc(SO_3H)_4)_2$, $K_D = 9.3 \times 10^7$ M [116]) but can be destroyed by the addition of alcohol [116] or detergent (e.g. Triton X-100) [111] (Fig. 13). $H_2TAP(C_6H_4SO_3H)_8$ containing twice as many SO_3H groups does not aggregate in water [113]. Owing to ionization of the SO_3H groups the aqueous solutions of these ligands are slightly acidic (pH 4–5). Upon increasing the pH, acid ionization can proceed with formation of monoanions and dianions: HAP^- and AP^{2-}. For $H_2Pc(SO_3H)_4$ in water, $pK_1^{293\,K} = 9.6$ and the removal of the second proton proceeds only at pH > 12 [116]. For monosulphophthalocyanine $H_2Pc(SO_3H)$ $pK_1^{293\,K} = 10.73$ (in DMSO) determined by Sheinin et al. [74], also showing that values of pK_1 and pK_2 are very close. Quantitative data on sulpho derivatives of tetraazaporphyrin ligands are absent, but on the basis of UV–visible spectra it was concluded that the unionized form $H_2TAP(C_6H_4SO_3H)_8$ exists in the interval $3 < pH < 9$ and, in the pH region 9–11.8, full ionization of N—H bonds proceeds and the dianion $[TAP(C_6H_4SO_3H)_8]^{2-}$ appears [112]. The basic properties of tetraazaporphyrin ligands are very weak even in the absence of electron-withdrawing $-SO_3H$ groups. As was shown for H_2TAP and H_2TAPPh_8, the *meso*-nitrogen atoms are more basic than intracyclic nitrogen atoms and they enter first

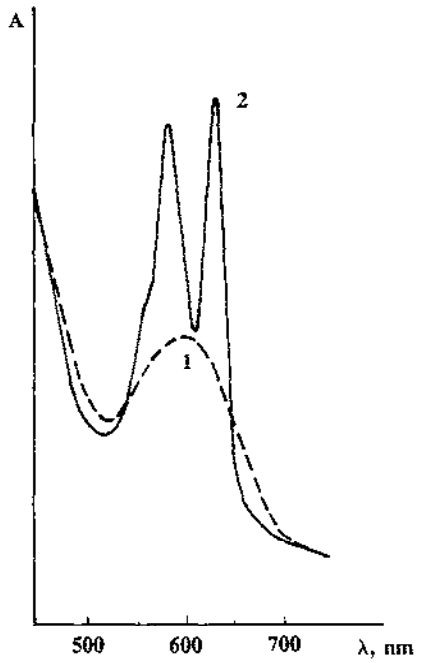

Fig. 13. UV–visible spectra of $H_2TAP(SO_3H)_4$ in water; curve 1, associated form; curve 2, monomeric form in the presence of 4% Triton X-100.

into a strong interaction with acids forming, in an H_2SO_4–AcOH mixture ion–ionic associates $H_2APH^+ \cdots A^-$ ($pK_{III} = -0.15$ and -3.08 respectively) [80,83]. Acid–base interaction with intracyclic nitrogen atoms is restricted by acid solvation and their protonation can proceed only in very strong acid media ($pK_{IV} = -4 - -5$ and -8.8 respectively).

3.3.2. The influence of ligand structure

The introduction of electron-withdrawing sulpho groups drastically increases the reactivity of tetraazaporphyrin ligands and complex formation with $H_2TAP(SO_3H)_4$, unlike H_2TAP, in alcohols, proceeds instantaneously. The reaction is tangibly retarded in the presence of acetic acid (Table 8). In water solution, metal ions exist as hexahydrated cations $[M(H_2O)_6]^{2+}$ and metal incorporation in $H_2TAP(SO_3H)_4$ proceeds much more slowly than in pure alcohols where metal acetates form non-ionized solvates: $[M(OAc)_2(EtOH)_4]$. This is due to the larger stability of the aqua complex than solvate. Ionization of $-SO_3H$ groups in water reduces the pH and is also responsible for retardation of the reaction. Nevertheless the introduction of $-SO_3H$ groups very strongly increases the reactivity of the ligand in complex formation with Zn(II), and also with complexes of usually inert Mg(II) and Sr(II) which complex with high rates in mild conditions. $H_2TAP(SO_3H)_4$ having electron-withdrawing $-SO_3H$ groups located directly in the pyrrole rings exhibits higher complexation rates than $H_2TAP(C_6H_4SO_3H)_8$ or $H_2Pc(SO_3H)_4$ where the $-SO_3H$

Table 8
Kinetic parameters for complexation of water-soluble sulpho-substituted tetraazaporphyrin and phthalocyanine ligands with metal acetates

Complex	Solvent	$k_v^{298\ K}$ ($s^{-1}\ M^{-1}$)	E_a ($kJ\ mol^{-1}$)	$\Delta S^{\neq}$ ($J\ mol\ K^{-1}$)
$ZnTAP(SO_3H)_4$	EtOH or MeOH	Very quick		
	EtOH + 7.5% AcOH	0.38	44	−170
	MeOH + 7.5% AcOH	1.20	44	−176
	H_2O[a]	15.17	41	−170
$MgTAP(SO_3H)_4$	H_2O[a]	5.22	55	−137
$SrTAP(SO_3H)_4$	H_2O[a]	0.45	40	−221
$ZnTAP(C_6H_4SO_3H)_6$	H_2O[a], pH 5	0.217		
	H_2O, pH 5	1.067	38	−189
	H_2O, pH 4.5	0.587	38	−195
$MgTAP(C_6H_4SO_3H)_8$	H_2O, pH 5	0.032	55	−162
	H_2O, pH 4	0.0059	55	−176
$ZnPc(SO_3H)_4$[b]	H_2O, pH 4.5	0.52	106	+30
$CuPc(SO_3H)_4$[b]	H_2O, pH 4.5	190	56	−89

[a] In the presence of 4% Triton X-100 which retards the reaction of about five times.
[b] Calculated on the basis of data from [108].
Uncertainties in k_v and E_a are less than 10%, and in $\Delta S^{\neq} \pm 10\ J\ mol\ K^{-1}$.

groups are isolated by benzene rings. Tetrasulphophthalocyanine in water solution appears to be less active than the tetrabutyl-substituted derivative in pyridine. Values of E_a and $\Delta S^{\neq}$ for the phthalocyanine ligand are substantially higher than for tetraazaporphyrin ligands. This is probably due to its more rigid skeleton. In tetraazaporphyrins, the skeleton is more flexible to deformation and decreasing the activation energy, E_a, also provides better conditions for the solvation of the transition state which reduces $\Delta S^{\neq}$.

3.3.3. Mechanism of complexation

The reaction of complex formation is first order in metal cation in the case of $H_2TAP(SO_3H)_4$ [112,113] and $H_2Pc(SO_3H)_4$ [108] and proceeds according to the bimolecular mechanism (9). The supposition made by Schitter and Bernauer [108] that removal of the internal proton and the formation of the monocation $[HPc(SO_3H)_4]^-$ is the rate-determining step is erroneous. Studying the influence of pH on the UV–visible spectra of $H_2Pc(SO_3H)_4$, they noticed that introduction of a base into the solution until pH > 10 leads to slowly developing spectroscopic changes interpreted as the formation of the monocation. This slow kinetic process was assigned to the acid ionization process. In fact, the removal of the proton from the reaction centre and formation of monoanions and dianions proceeds instantaneously [74,75] and cannot be measured by conventional kinetic methods. The usual rate for proton transfer processes is $k > 10^8\ s^{-1}\ M^{-1}$ [117]. Bernauer and Fallab [115], using water solutions where according to their data a very stable dimer exists, obtained rate constants reflecting the monomerization process promoted by hydrox-

ide anions and not ionization. Further it is $H_2Pc(SO_3H)_4$ and not $[HPc(SO_3H)_4]$ that takes part in complexation with metal ions in the pH range $4 < pH < 6$ investigated [108].

The complexation of $H_2TAP(C_6H_4SO_3H)_8$ was, unlike tetrasulpho derivatives, zero order in metal ion and proceeds in accordance with the monomolecular rate law [113]. Since, in acid media, the formation of an intermediate complex with *meso*-nitrogen atoms seems unlikely, the zero order in metal ion is explained more probably by the association of cations $[M(H_2O)_6]^{2+}$ with the octa-anion $[H_2TAP(C_6H_4SO_3)_8]^{8-}$ followed by the migration of the cation to the reaction centre in the solvent cage.

3.3.4. The influence of pH

The influence of the acidity of the medium on the reaction rate was studied for complexation of $H_2TAP(C_6H_4SO_3H)_8$ with Mg^{2+} and Zn^{2+} cations [112]. The reaction accelerates considerably upon increase in pH with simultaneous decreases in E_a and $\Delta S^{\neq}$ (Table 9). The rate constants do not change proportionally to the OH^- concentration; their dependence on pH is more complicated. The acceleration of complexation with change in pH from 3 to 9 units is not connected with equilibrium of monoanion or dianion formation as was supposed by Schiller and Bernauer [108]. In this case the activation parameters should not depend in this way on pH.

Table 9
Kinetic parameters for formation of $MTAP(C_6H_4SO_3H)_8$ water at different pH ($[H_2AP]^0 = 1.17 \times 10^{-5}$ M, $[M(OAc)_2]^0 = 3.75 \times 10^{-4}$ M) [112]

pH	$k_v^{298\ K} \times 10^4$ (s^{-1})	E_a (kJ mol^{-1})	$\Delta S \neq$ (J $mol\ K^{-1}$)
$MgTAP(C_6H_4SO_3H)_8$			
3	0.0009	92±8	−76±24
4	0.022	55±6	−176±18
5	0.12	55±5	−162±15
6	0.30	45±4	−186±13
7	6.12	24±3	−234±10
8	7.72	25±2	−228±10
9	7.32	30±3	−212±9
$ZnTAP(C_6H_4SO_3H)_8$			
3	0.54	50±2	−167±7
3.5	0.65	54±5	−152±17
4	0.84	47±3	−172±9
4.5	2.20	38±3	−195±9
5	4.00	38±5	−189±18
5.5	7.30	32±3	−205±10
6.5	21.6	7±1	−280±4
7	24.1	6±1	−282±4
7.5	34.1	5±1	−284±4

Uncertainties in k_v are less than 10%.

The first reason is the formation of ion–molecular associates of hydroxide ions with hydrogen atoms of the reaction centre >NH···OH; promoting their subsequent removal; the second is the accumulation of hydroxohydrates $[M(OH)(H_2O)_5]^+$ supplying OH^- anions directly into the reaction centre. On the contrary, lowering the pH strengthens the acid solvation of the donor centres of the ligand (nitrogen atoms) and this leads to its localized structure which is less active in complexation and has higher activation parameter values. It is note worthy that as the pH increases, i.e. a transition from the LS to the US structure, there is a levelling of complexation rates with Mg^{2+} and Zn^{2+}. For the LS structure at pH 3 they differ by a factor of 600 whereas for the US structure at pH 7 by a factor of 4. The more active substrate is less selective.

3.3.5. The influence of organic solvent addition

The complexation of $H_2TAP(C_6H_4SO_3H)_8$ with Zn acetate in water with addition of organic solvents was studed by Petrov and coworkers [113]. In the presence of small additions (0.05 M) of DMSO, AcOH, EtOH, MeCN, HMPTA, DMF or pyridine, the aquamonosolvate $[Zn(H_2O)_5solv]^{2+}$ prevails in solution. The addition of solvent with pronounced basic (pyridine) or acidic (AcOH) properties causes the largest changes in complexation rates and activation parameters (Table 10). The addition of AcOH retards the reaction by 80 times, simultaneously drastically increasing E_a and also $\Delta S^{\neq}$ values. The addition of pyridine increases the complexation rate by 2.6 times, leaving E_a and $\Delta S^{\neq}$ values unchanged. The influence of the pyridine and acetic acid additions is similar to the change in pH. In the presence of AcOH, the reaction centre has a less reactive LS structure whereas, in the presence of pyridine, the US structure exists as it does in pure water. As usual, pyridine assists in the removal of the NH protons in the process of complexation. The addition of solvents without distinct acidic or basic properties does not change the pH and the reaction is retarded only slightly by solvents with a higher donor number. On the contrary, the influence on the activation parameters is very large. Such additions do not change the structure of the reaction centre but change the structure of the metal

Table 10
Kinetic parameters for the formation of $ZnTAP(C_6H_4SO_3H)_8$ in water with addition of 0.05 M organic solvents ($[H_2AP]^0 = 1 \times 10^{-5}$ M; $[Zn(OAc)_2]^0 = 6.0 \times 10^{-4}$ M) [113,114]

Solvent	Donor number	$k_v^{298\,K} \times 10^4$ (s^{-1})	E_a (kJ mol^{-1})	$\Delta S^{\neq}$ (J $mol\ K^{-1}$)
H_2O	18.0	24.1±0.9	5±1	−285±30
Pyridine	33.1	62.7±1.2	3±1	−285±30
AcOH	17.1	0.297±0.010	68±2	−112±6
DMSO	29.8	22.4±0.5	17±1	−247±4
EtOH	19.6	14.7±0.4	26±1	−220±14
MeCN	14.1	14.2±0.4	37±4	−184±12
DMF	26.6	12.2±0.5	24±2	−228±7
HMPTA	38.8	8.3±0.4	43±2	−168±7

salt transforming it from a hexahydrate to an aquamonosolvate. It is the difference between the strengths of these M—H_2O and M—solv bonds that determines activation parameters.

4. Conclusions

Aza substitution has great impact on the structure of the reaction centre of porphyrin ligands and to a large extent determines the structure and properties of phthalocyanines. It decreases the dimensions of the coordination cavity and increases the acidity of the N–H bonds, creating conditions for the formation of strong intramolecular hydrogen bonds in tetraazaporphyrins and phthalocyanines. The nature of the N—H bonds depends on intermolecular interactions with the environment and can differ in the vapour, solid and solution phases. The use of different models of the reaction centre structure — localized, hydrogen bonded and unlocalized — is helpful in understanding and explaining the properties of these ligands, especially in solution. Kinetic studies of metalloazaporphyrin formation carried out in different organic solvents and also in water media have shown that aza substitution leads to a considerable increase in the reactivity of these porphyrin-type ligands in complexation with metal salts. The solvation of the azaporphyrin reaction centre is a crucial factor determining their reactivity in complexation. In strongly coordinating solvents such as pyridine where the azaporphyrin ligands have a delocalized reaction centre structure, they are much more active in complexation than are common porphyrins. On the contrary, in weakly coordinating but proton-donating solvents (acetic acid, and alcohols) the reaction centre attains a localized structure and complexation reactivity becomes comparable or even less than that of porphyrins.

References

[1] P. Hambright, Coord. Chem. Rev., 6 (1971) 247.
[2] F.R. Longo, E.M. Brown, D.J. Quimby, A.D. Adler and M. Meot-Ner, Ann. N.Y. Acad. Sci., 206 (1973) 420.
[3] W. Scheider, Struct. Bonding, 23 (1975) 123.
[4] B.D. Berezin, Coordination Compounds of Porphyrins and Phthalocyanine, Wiley, New York, 1981.
[5] B.D. Berezin and N.S. Enikolopyan (eds.), Porfiriny: Struktura, Svoystva, Sintez (Porphyrins: Structure, Properties, Synthesis), Nauka, Moscow, 1985, p. 49.
[6] B.D. Berezin and N.S. Enikolopyan, Metalloporfiriny (Metalloporhyrins) Nauka, Moscow, 1988.
[7] B.D. Berezin and O.G. Khelevina, in B.D. Berezin and N.S. Enikolopyan (eds.), Porfiriny: Struktura, Svoystva, Sintez (Porphyrins: Structure, Properties, Synthesis), Nauka, Moscow, 1985, p. 83.
[8] L.E. Webb and E.B. Fleischer, J. Chem. Phys., 43 (1965) 3100.
[9] B. Chen and A. Tulinsky, J. Am. Chem. Soc., 94 (1972) 4144.
[10] M.J. Hamor, T.A. Hamor and J.L. Hoard, J. Am. Chem. Soc., 86 (1964) 1938.
[11] S.J. Silvers and A. Tulinsky, J. Am. Chem. Soc., 89 (1967) 3331.
[12] A. Tulinsky, Ann. N.Y. Acad. Sci., 206 (1973) 47.

[13] J.W. Laucher and J.A. Ibers, J. Am. Chem. Soc., 95 (1973) 5148.
[14] I.M. Das and B. Chandhuri, Acta Crystallogr., Sect. B, 28 (1972) 579.
[15] J.M. Robertson, J. Chem. Soc., (1936) 1195.
[16] B.F. Hoskins, S.A. Mason and J.C.B. White J. Chem. Soc., Chem. Commun., (1969) 554.
[17] I. Woodward, J. Chem. Soc., (1940) 601.
[18] J.M. Robertson, J. Chem. Soc., (1939) 1809.
[19] A.L. Balch, M.M. Olmstead and N. Safari, Inorg. Chem., 32 (1993) 291.
[20] C.B. Velazques, G.A. Fox, W.E. Broderick, K.A. Andersen, O.P. Anderson, A.G.M. Barret and B.M. Hoffman, J. Am. Chem. Soc., 114 (1992) 7416.
[21] J.P. Fitzgerald, B.S. Haggerty, A.L. Rheingold, L. May and G.A. Brever, Inorg. Chem., 31 (1992) 2006.
[22] H. Masuda, T. Taya, K. Osaki, H. Sugimoto, Z.-I. Yoshida and H. Ogoshi, Inorg. Chem., 19 (1980) 950.
[23] J.L. Hoard, G.H. Cohen and N.D. Glick, J. Am. Chem. Soc., 89 (1967) 1992.
[24] A. Ulman, J. Galucci, D. Fisher and J.A. Ibers, J. Am. Chem. Soc., 102 (1980) 6852.
[25] J. Martinsen, L.J. Pace, T.E. Phillips, B.M. Hoffman and J.A. Ibers, J. Am. Chem. Soc., 104 (1982) 83.
[26] C.J. Schramm, R.P. Scaringe, D.R. Stojakovic, B.M. Hoffman, J.A. Ibers and T.J. Mark, J. Am. Chem. Soc., 102 (1980) 6702.
[27] S.M. Palmer, J.L. Stanton, N.K. Jaggi, B.M. Hoffman, J.A. Ibers and L.H. Schwarz, Inorg. Chem., 24 (1985) 2040.
[28] C. Weiss, H. Kobayashi and M. Gouterman, J. Mol. Spectrosc., 16 (1965) 415.
[29] A.M. Schaffer and M. Gouterman, Theor. Chim. Acta, 25 (1972) 62.
[30] V.M. Mamaev, I.P. Gloriozov and L.G. Boyko, Zh. Strukt. Khim., 20 (1979) 332.
[31] S.S. Dvornikov, V.N. Knyukshto, V.A. Kuz'mitsky, A.M. Shul'ga and K.N. Solovyov, J. Lumin., 23 (1981) 373.
[32] E. Orti, M.C. Piqueras, R. Crespo and J.L. Bredas, Chem. Mater., 2 (1990) 110.
[33] Z. Berkovitch-Yellin and D.E. Ellis, J. Am. Chem. Soc., 103 (1981) 6066.
[34] P.A. Stuzhin, Thesis, Institute of Chemical Technology, Ivanovo, 1985.
[35] Y. Niwa, H. Kobayashi and T. Tsuchijya, J. Chem. Phys., 60 (1974) 799.
[36] V.N. Kopranenkov, A.M. Vorotnikov, T.M. Ivanova and E.A. Luk'yanets, Khim. Geterotsikl. Soedin., (1988) 1351.
[37] G.M. Badger, R.L. Harris, R.A. Jones and J.M. Sasse, J. Chem. Soc., (1962) 4329.
[38] L.L. Gladkov, A.T. Gradyuschko, A.M. Shul'ga, K.N. Solovyov and A.S. Starukhin, J. Mol. Spectrosc., 47 (1978) 463.
[39] K.N. Solovyov, L.L. Gladkov, A.S. Starukhin and S.F. Shkirman, Spektroskopiya Porfirinov: Kolebatel'nye Sostoyaniya (Spectroscopy of Porphyrins: Vibration States), Nauka i Tekhnika, Minsk, 1985.
[40] V.A. Kuz'mitsky and K.N. Solovyov, J. Mol. Spectrosc., 65 (1980) 219.
[41] V.P. Pinchuk, V.A. Korobski and V.V. Lobanov, Teor. Eksp. Khim., 20 (1984) 206.
[42] (a) K.N. Solovyov, V.A. Mashenkov and A.T. Gradyushko, Zh. Prikl. Spektrosk., 13 (1970) 339; (b) C.B. Storm and J. Teklu, J. Am. Chem. Soc., 94 (1972) 1745; (c) G.D. Egorova, K.N. Solovyov and A.M. Shul'ga, Teor. Eksp. Khim., 11 (1975) 77; (d) R.J. Abraham, G.E. Hawkes and K.V. Smith, Tetrahedron Lett., (1974) 1483.
[43] V.M. Mamaev, S.Ya. Ishtchenko and I.P. Gloriozov, Izv. Vyssh. Uchebn. Zaved., Khim. Khim. Tekhnol., 32(1) (1989) 3.
[44] B.D. Berezin, Izv. Vyssh. Uchebn. Zaved., Khim. Khim. Tekhnol., 2 (1959) 165.
[45] B.D. Berezin, Zh. Fiz. Khim., 39 (1965) 321.
[46] E.B. Fleischer, Acc. Chem. Res., 3 (1970) 105.
[47] J.N. Sharp and M. Lardon, J. Phys. Chem., 72 (1968) 3230.
[48] L. Edwards and M. Gouterman, J. Mol. Spectrosc., 33 (1970) 292.
[49] E.A. Lucia, C.P. Marino and F.D. Verderame, J. Mol. Spectrosc., 26 (1968) 133.
[50] E.A. Lucia and F.D. Verderame, J. Chem. Phys., 48 (1968) 2674.
[51] K.N. Solovyov, O stroenii porfina i ego proizvodnykh (About the structure of porphine and its derivatives), Preprint, Institute of Physics, Akademii Nauk Belorusskoi SSR, Minsk, 1969.

[52] I. Chen, J. Mol. Spectrosc., 23 (1967) 131.
[53] V.M. Mamaev, I.P. Gloriozov and V.V. Orlov, Izv. Vyssh. Uchebn. Zaved., Khim. Khim. Tekhnol., 25 (1982) 1317.
[54] V.M. Mamaev and I.P. Gloriozov, Abstracts of the 14th All-Union Chugaev's Conf. Part I, Ivanovo, 1981, p. 17.
[55] Y. Niwa, H. Kobayashi and T. Tsuchiya, Inorg. Chem., 13 (1974) 2891.
[56] M.V. Zeller and R.G. Hayes, J. Am. Chem. Soc., 95 (1973) 3855.
[57] B. Dudreva and S. Grande, J. Phys. (Paris), Colloq. C2, 33 (1972) 183.
[58] B.H. Meyer, C.B. Storm and W.L. Earl, J. Am. Chem. Soc., 108 (1986) 6072.
[59] R.D. Kendrick, S. Fridrich, B. Wehrle, H.-H. Limbach and C.S. Yannoni, J. Magn. Reson., 65 (1985) 159.
[60] B. Wehrle, H.-H. Limbach, M. Köcher, O. Ermer and E. Vogel, Angew. Chem., 99 (1987) 914.
[61] E.D. Becker, R.B. Bradley and C.J. Watson, J. Am. Chem. Soc., 83 (1961) 3743.
[62] C.C. Leznoff, in C.C. Leznoff and A.B.P. Lever (eds.), Phthalocyanines: Properties and Applications, VCH, New York, 1989, p. 1.
[63] N.A. Andronova and E.A. Luk'yanets, Zh. Prikl. Spektrosk., 20 (1974) 312.
[64] M. Hanack, J. Metz and G. Pawlowski, Chem. Ber., 115 (1982) 2836.
[65] S.M. Marcuccio, P.I. Svirskaya, S. Greenberg, A.B.P. Lever, C.C. Leznoff and K.B. Tomer, Can. J. Chem., 63 (1985) 3057.
[66] V.N. Kopranenkov, E.A. Tarkhanova and E.A. Luk'yanets, Zh. Org. Khim., 15 (1979) 642.
[67] N. Yu. Borovkov and A.S. Akopov, Zh. Strukt. Khim., 28 (1987) 175.
[68] Yu.B. Vysotsky, V.A. Kuzmitsky and K.N. Solovyov, Theor. Chim. Acta, 59 (1981) 467.
[69] (a) Yu.K. Grishin, O.A. Subbotin, Yu.A. Ustynyuk, V.N. Kopranenkov, L.S. Goncharova and E.A. Luk'yanets, Zh. Strukt. Khim., 20 (1979) 352; (b) V.N. Kopranenkov, D.B. Askerov, A.M. Shul'ga and E.A. Luk'yanets, Khim. Geterotsikl. Soedin., (1988) 1261.
[70] Yu.K. Grishin, V.N. Kopranenkov and L.S. Goncharova, Zh. Prikl. Spektrosk., 32 (1980) 360.
[71] J. Fitzgerald, W. Taylor and H. Owen, Synthesis, (1991) 686.
[72] (a) O.G. Khelevina, N.V. Chizhova and B.D. Berezin, Zh. Org. Khim., 27 (1991) 805; (b) O.G. Khelevina, N.V. Chizhova and B.D. Berezin, Khim. Geterotsikl. Soedin., (1992) 619.
[73] V.B. Sheinin, V.G. Andrianov and B.D. Berezin, Zh. Org. Khim., 20 (1984) 2192, 2224.
[74] V.B. Sheinin, V.G. Andrianov, B.D. Berezin and T.A. Koroleva, Zh. Org. Khim., 21 (1985) 1564.
[75] V.B. Sheinin, B.D. Berezin, O.G. Khelevina, P.A. Stuzhin and F.Yu. Telegin, Zh. Org. Khim., 21 (1985) 1571.
[76] O.G. Khelevina, N.V. Chizhova and B.D. Berezin, Koord. Khim., 17 (1991) 400.
[77] V.I. Smirnov, A.I. V'yugin and A.G. Krestov, Zh. Fiz. Khim., 63 (1989) 2245.
[78] G.M. Trofimenko and B.D. Berezin, Russ. J. Inorg. Chem., 38 (1993) 971.
[79] B.D. Berezin, Teor. Eksp. Khim., 9 (1973) 500.
[80] B.D. Berezin, P.A. Stuzhin and O.G. Khelevina, Khim. Geterotsikl. Soedin., (1986) 1677.
[81] S. Gaspard, M. Verdaquer and R. Viovy, C.R. Acad. Sci. Paris, Ser. C, 277 (1973) 821.
[82] (a) S.S. Iodko, O.L. Kaliya, O.L. Lebedev and E.A. Luk'yanets, Koord. Khim., 5 (1979) 611; (b) P.A. Bernstein and A.B.P. Lever, Inorg. Chim. Acta, 200 (1992) 543.
[83] B.D. Berezin, O.G. Khelevina and P.A. Stuzhin, Zh. Prikl. Spektrosk., 46 (1987) 809.
[84] C.S. Velazques, W.E. Broderic, M. Sabat, A.G.M. Barret and B.M. Hoffman, J. Am. Chem. Soc., 112 (1990) 7408.
[85] B.D. Berezin, O.G. Khelevina, N.D. Gerasimova and P.A. Stuzhin, Zh. Fiz. Khim., 56 (1982) 2768.
[86] B.D. Berezin, O.G. Khelevina and P.A. Stuzhin, Zh. Fiz. Khim., 59 (1985) 2181.
[87] P.A. Stuzhin, O.G. Khelevina, S.S. Metel'kova and B.D. Berezin, Izv. Vyssh. Uchebn. Zaved., Khim. Khim. Tekhnol., 29(5) (1986) 19.
[88] P.A. Stuzhin, O.G. Khelevina and B.D. Berezin, Zh. Fiz. Khim., 61 (1987) 82.
[89] E.B. Karavaeva, T.I. Potapova and B.D. Berezin, Izv. Vyssh. Uchebn. Zaved., Khim. Khim. Tekhnol., 21 (1978) 1099.
[90] O.G. Khelevina, B.D. Berezin, O.A. Petrov and A.V. Glazunov, Koord. Khim., 16 (1990) 1047.
[91] N.Yu. Borovkov and A.S. Akopov, Koord. Khim., 10 (1984) 455.

[92] O.G. Khelevina, P.A. Stuzhin, A.V. Głazunov and B.D. Berezin, Proc. 5th All-Union Conf. on Chemistry of Non-aqueous Solvents, Nauka, Moscow, 1985, p. 122.
[93] O.G. Khelevina, S.V. Timofeeva, B.D. Berezin and S.I. Vagin, Zh. Fiz. Khim., 68 (1994) 1423.
[94] S.V. Kharitonov, B.D. Berezin, T.I. Potapova and R.A. Petrova, Zh. Fiz. Khim., 57 (1983) 1680.
[95] O.G. Khelevina, P.A. Stuzhin and B.D. Berezin, Izv. Vyssh. Uchebn. Zaved., Khim. Khim. Tekhnol., 32(12) (1989) 44.
[96] O.V. Malkova, V.G. Andrianov, B.D. Berezin and G.M. Trofimenko, Izv. Vyssh. Uchebn. Zaved., Khim. Khim. Tekhnol., 36(4) (1993) 116.
[97] N.Yu. Borovkov and A.S. Akopov, Zh. Obshch. Khim., 55 (1985) 2549.
[98] B.D. Berezin, Russ. Chem. Rev., 60 (1991) 996.
[99] M. Whalley, J. Chem. Soc., (1961) 866.
[100] S.V. Vul'fson, O.A. Lebedev and E.A. Luk'yanets, Zh. Prikl. Spektrosk., 17 (1972) 903.
[101] O.G. Khelevina, P.A. Stuzhin and B.D. Berezin, Zh. Fiz. Khim., 60 (1986) 1881.
[102] W. Libus, S. Hoffman, M. Kluczkowski and H. Twardowska, Inorg. Chem., 19 (1980) 1625.
[103] J.K. Kochi and R.V. Subramaninan, Inorg. Chem., 4 (1965) 1527.
[104] H. Crasdalien and I. Svare, Acta Chem. Scand., 25 (1971) 1089.
[105] O.A. Golubchikov, O.I. Koifman and B.D. Berezin, Zh. Fiz. Khim., 50 (1976) 1469.
[106] S.J. Baum and R.A. Plane, J. Am. Chem. Soc., 88 (1966) 910.
[107] O.G. Khelevina, N.V. Chizhova and B.D. Berezin, Patent SU 1594178, Chem. Abstr., 114 (1991) 156315q.
[108] I. Schiller and K. Bernauer, Helv. Chim. Acta, 56 (1963) 3002.
[109] O.G. Khelevina, N.V. Chizhova and B.D. Berezin, Zh. Org. Khim., 28 (1992) 160.
[110] N.V. Chizhova, O.G. Khelevina, O.A. Petrov and B.D. Berezin, Abstracts of the 5th All-Union Conf. on Chemistry of the Nitrogen-containing Heterocycles, Chernogolovka, 1991, 1991, p. 245; N.V. Chizhova, Thesis, Institute of Chemical Technology, Ivanovo, 1990.
[111] S.V. Timofeeva, O.G. Khelevina and B.D. Berezin, Zh. Fiz. Khim., 67 (1993) 1798.
[112] O.A. Petrov, O.G. Khelevina and B.D. Berezin, Izv. Vyssh. Uchebn. Zaved., Khim. Khim. Tekhnol., 34(5) (1991) 25.
[113] B.D. Berezin, O.A. Petrov and O.G. Khelevina, Koord. Khim., 17 (1991) 1124.
[114] O.A. Petrov, O.G. Khelevina and B.D. Berezin, Koord. Khim., 20 (1994) 270.
[115] K. Bernauer and S. Fallab, Helv. Chim. Acta, 44 (1961) 1287.
[116] K. Bernauer and S. Fallab, Helv. Chim. Acta, 45 (1962) 2487.
[117] E. Chiang, A.L. Kresle and J.F. Holzwarth, J. Chem. Soc., Chem. Commun., (1982) 1203.